arXiv:1605.06675v1 [hep-ph] 21 May 2016

Higgs Boson Mass and Muon $g-2$ with Strongly Coupled Vector-like Generations

Michinobu Nishida[1] and Koichi Yoshioka[2]

[1] *Department of Physics, Keio University, Yokohama 223-8522, Japan*
[2] *Osaka University of Pharmaceutical Sciences, Takatsuki 569-1094, Japan*

(May 2016)

Abstract

We study the Higgs boson mass and the muon anomalous magnetic moment (the muon $g-2$) in a supersymmetric standard model with vector-like generations. The infrared physics of the model is governed by strong renormalization-group effects of the gauge couplings. That leads to sizable extra Yukawa couplings of Higgs doublets between the second and vector-like generations in both quark and lepton sectors. It is found with this property that there exist wide parameter regions where the Higgs boson mass and the muon $g-2$ are simultaneously explained.

1 Introduction

The discovery of the Higgs boson by the ATLAS and CMS collaborations of the LHC gives big impacts on particle physics [1, 2]. All the elementary particles of the Standard Model (SM) with gauge symmetry SU(3) × SU(2) × U(1) are experimentally confirmed.

Supersymmetry (SUSY) provides one of the most attractive candidates for the theory beyond the SM. In the Minimal Supersymmetric Standard Model (MSSM) with low-energy supersymmetry [3], three gauge couplings are unified at a high-energy scale and the lightest superpartner of SM particles would be dark matter in the Universe. Furthermore the electroweak symmetry breaking is naturally triggered around the Fermi scale [4] and is stabilized by the cancellation of quantum corrections.

We focus on two important physical quantities: the Higgs boson mass and the muon anomalous magnetic moment (the muon $g-2$). The Higgs boson mass was determined to be around 125 GeV by the LHC experiments. In the MSSM, it is well known that the Higgs mass is below the Z boson mass at tree level and can be raised by the radiative correction from the $\mathcal{O}(1)$ top Yukawa coupling [5, 6]. The Higgs mass generally becomes large when the SUSY breaking (in the top sector) is large since the cancellation of divergences is weakened. The muon $g-2$, which is defined by $a_\mu = (g-2)_\mu/2$, shows the discrepancy between the experimental result and the SM prediction that indicates new physics beyond the SM. The discrepancy is above 3 sigma and quantified as $\Delta a_\mu \equiv a_\mu(\mathrm{exp}) - a_\mu(\mathrm{SM}) = (28.1 \pm 8.0) \times 10^{-10}$ [7, 8]. The muon $g-2$ generally becomes small when the SUSY breaking (in the muon sector) is large [9, 10] due to the decoupling property. It is noticed that these two quantities have the opposite dependences on SUSY breaking (the masses of superpartners). This fact leads to a problem in the MSSM that two experimental results are not simultaneously explained for universal SUSY-breaking parameters, e.g. the minimal supergravity mediation [11].

In this work, we consider the effect of extra vector-like generations to the above problem. It is known that light vector-like matter fermions are consistent with the precision electroweak measurements, while only the 4th (chiral) generation is not [12]. Further, with (a pair of) vector-like generations, the gauge coupling unification is preserved [13,14]. The gauge couplings in high-energy regime are larger than those of the MSSM and hence the renormalization-group (RG) running is governed by the gauge sector. As a result, the ratios of Yukawa and gauge couplings have strong convergence to their infrared-fixed point values. It is therefore possible to determine Yukawa (and other) couplings at low-energy [15] which are insensitive to high-energy initial values with the strong convergence property [14, 16]. In Ref. [17], we show that the fixed-point behavior determines the matrix forms of Yukawa couplings for the up-type, down-type quarks and charged leptons with the vector-like generations. A notable fact in these Yukawa matrices is that the Higgs boson and the muon have sizable couplings to the vector-like generations. In this paper, we focus on these Yukawa

matrices and evaluate the contributions of vector-like generations to the Higgs boson mass and the muon $g-2$.

The organization of this paper is as follows. In Section 2, we introduce vector-like generations and explain our model. The RG behaviors of gauge and Yukawa couplings are discussed and the realistic forms of Yukawa matrices are determined by the fixed-point property. In Section 3, we give the analytic formulae of the Higgs boson mass and the muon $g-2$ in the model. In Section 4, we first describe the RG property of SUSY-breaking parameters on which the Higgs mass and the muon $g-2$ depend. We then show the parameter regions where the Higgs mass and the muon $g-2$ are explained simultaneously, and compare our model with the MSSM. The final section is devoted to the conclusion.

2 Model

We introduce a pair of vector-like generations (i.e. the 4th and 5th ones) to the MSSM. The (super)fields for the MSSM part are

$$Q_i,\ u_i,\ d_i,\ L_i,\ e_i, \quad (i=1,\cdots,3) \tag{2.1}$$

$$H_u,\ H_d, \tag{2.2}$$

where Q_i and L_i are the SU(2) doublets of quarks and leptons, u_i, d_i and e_i are the SU(2) singlets of up-type, down-type quarks and charged leptons, respectively. The Higgs doublets are denoted by H_u and H_d. The (super)fields for the vector-like generation part are

$$Q_4,\ u_4,\ d_4,\ L_4,\ e_4, \tag{2.3}$$

$$\bar{Q},\ \bar{u},\ \bar{d},\ \bar{L},\ \bar{e}, \tag{2.4}$$

$$\Phi. \tag{2.5}$$

The quantum charges of these superfields are summarized in Table 2.1. The chiral superfields in (2.3) have the same charges as the MSSM generations, and those in (2.4) have the opposite charges. These pairs with opposite charges are called vector-like generations. The field Φ in (2.5) is a gauge singlet under the SM gauge transformation. The superpotential in the model is

$$\begin{aligned} W = &\sum_{i,j=1,\cdots,4} \Big(\boldsymbol{y}_{u_{ij}} u_i Q_j H_u + \boldsymbol{y}_{d_{ij}} d_i Q_j H_d + \boldsymbol{y}_{e_{ij}} e_i L_j H_d \Big) + \mu_H H_u H_d \\ &+ y_{\bar{u}}\, \bar{u}\bar{Q} H_d + y_{\bar{d}}\, \bar{d}\bar{Q} H_u + y_{\bar{e}}\, \bar{e}\bar{L} H_u + M\Phi^2 + Y\Phi^3 \\ &+ \sum_{i=1,\cdots,4} \Big(Y_{Q_i} \Phi Q_i \bar{Q} + Y_{u_i} \Phi u_i \bar{u} + Y_{d_i} \Phi d_i \bar{d} + Y_{L_i} \Phi L_i \bar{L} + Y_{e_i} \Phi e_i \bar{e} \Big). \end{aligned} \tag{2.6}$$

	SU(3)	(SU(2), U(1))
Q_4	$\mathbf{3}$	$(\mathbf{2}, \frac{1}{6})$
u_4	$\mathbf{3}^*$	$(\mathbf{1}, \frac{-2}{3})$
d_4	$\mathbf{3}^*$	$(\mathbf{1}, \frac{1}{3})$
L_4	$\mathbf{1}$	$(\mathbf{2}, \frac{-1}{2})$
e_4	$\mathbf{1}$	$(\mathbf{1}, 1)$
$\bar{Q}$	$\mathbf{3}^*$	$(\mathbf{2}, \frac{-1}{6})$
$\bar{u}$	$\mathbf{3}$	$(\mathbf{1}, \frac{2}{3})$
$\bar{d}$	$\mathbf{3}$	$(\mathbf{1}, \frac{-1}{3})$
$\bar{L}$	$\mathbf{1}$	$(\mathbf{2}, \frac{1}{2})$
$\bar{e}$	$\mathbf{1}$	$(\mathbf{1}, -1)$
Φ	$\mathbf{1}$	$(\mathbf{1}, 0)$

Table 2.1: The chiral superfields and their quantum numbers under the SM gauge group.

The first two lines show the Yukawa interactions of five-generation matter fields. The interactions in the third line generate vector-like mass terms when the scalar component of Φ develops a vacuum expectation value. In addition, the soft SUSY-breaking terms are given by

$$\begin{aligned}
-\mathcal{L}_{\rm soft} = \Bigg[& \sum_{i,j=1,\cdots,4} (\boldsymbol{a}_{u_{ij}} \tilde{u}_i \tilde{Q}_j H_u + \boldsymbol{a}_{d_{ij}} \tilde{d}_i \tilde{Q}_j H_d + \boldsymbol{a}_{e_{ij}} \tilde{e}_i \tilde{L}_j H_d) + b_H H_u H_d \\
& + a_{\bar{u}}\, \tilde{\bar{u}} \tilde{\bar{Q}} H_d + a_{\bar{d}}\, \tilde{\bar{d}} \tilde{\bar{Q}} H_u + a_{\bar{e}}\, \tilde{\bar{e}} \tilde{\bar{L}} H_u + b_M \Phi^2 + A_Y \Phi^3 \\
& + \sum_{i=1,\cdots,4} (A_{Q_i} \Phi \tilde{Q}_i \tilde{\bar{Q}} + A_{u_i} \Phi \tilde{u}_i \tilde{\bar{u}} + A_{d_i} \Phi \tilde{d}_i \tilde{\bar{d}} + A_{L_i} \Phi \tilde{L}_i \tilde{\bar{L}} + A_{e_i} \Phi \tilde{e}_i \tilde{\bar{e}}) + \text{h.c.} \Bigg] \\
& + \tilde{Q}^\dagger \mathbf{m}_Q^2 \tilde{Q} + \tilde{L}^\dagger \mathbf{m}_L^2 \tilde{L} + \tilde{u}\, \mathbf{m}_u^2 \tilde{u}^\dagger + \tilde{d}\, \mathbf{m}_d^2\, \tilde{d}^\dagger + \tilde{e}\, \mathbf{m}_e^2 \tilde{e}^\dagger + m_{H_u}^2 H_u^* H_u + m_{H_d}^2 H_d^* H_d \\
& + m_{\bar{Q}}^2\, \tilde{\bar{Q}}^* \tilde{\bar{Q}} + m_{\bar{L}}^2 \tilde{\bar{L}}^* \tilde{\bar{L}} + m_{\bar{u}}^2\, \tilde{\bar{u}} \tilde{\bar{u}}^* + m_{\bar{d}}^2 \tilde{\bar{d}} \tilde{\bar{d}}^* + m_{\bar{e}}^2\, \tilde{\bar{e}} \tilde{\bar{e}}^* + m_\Phi^2 \Phi^* \Phi \\
& + \frac{1}{2} \big(M_3 \tilde{g} \tilde{g} + M_2 \tilde{W} \tilde{W} + M_1 \tilde{B} \tilde{B} + \text{h.c.} \big),
\end{aligned} \tag{2.7}$$

where the fields with tilde mean the scalar components of matter superfields, and $\tilde{g}, \tilde{W}$ and $\tilde{B}$ represent the gauginos for SU(3), SU(2) and U(1) gauge groups, respectively.

After the electroweak symmetry breaking, the mass matrices for the five-generation quarks and

leptons are given by

$$m_u = \begin{array}{c} \\ u_{1R} \\ \vdots \\ u_{4R} \\ u_{5R} \end{array} \begin{array}{c} \begin{array}{ccc} u_{1L} & \cdots & u_{4L} \quad u_{5L} \end{array} \\ \begin{pmatrix} & & \\ & \boldsymbol{y}_{u_{ij}} v_u & Y_{u_i} V \\ & & \\ & Y_{Q_j} V & y_{\bar{u}}\, v_d \end{pmatrix} \end{array}, \tag{2.8}$$

$$m_d = \begin{array}{c} \\ d_{1R} \\ \vdots \\ d_{4R} \\ d_{5R} \end{array} \begin{array}{c} \begin{array}{ccc} d_{1L} & \cdots & d_{4L} \quad d_{5L} \end{array} \\ \begin{pmatrix} & & \\ & \boldsymbol{y}_{d_{ij}} v_d & Y_{d_i} V \\ & & \\ & Y_{Q_j} V & y_{\bar{d}}\, v_u \end{pmatrix} \end{array}, \tag{2.9}$$

$$m_e = \begin{array}{c} \\ e_{1R} \\ \vdots \\ e_{4R} \\ e_{5R} \end{array} \begin{array}{c} \begin{array}{ccc} e_{1L} & \cdots & e_{4L} \quad e_{5L} \end{array} \\ \begin{pmatrix} & & \\ & \boldsymbol{y}_{e_{ij}} v_d & Y_{e_i} V \\ & & \\ & Y_{L_j} V & y_{\bar{e}}\, v_u \end{pmatrix} \end{array}, \tag{2.10}$$

where v_u, v_d and V are the vacuum expectation values of the scalar components of H_u,H_d and Φ, respectively. Here and hereafter, we denote the fields in the "5th" generation superfields (2.4) by those with the indices "5". For example, the fermions in the superfield $\bar{Q}$ are $(u_{5R})^C$ and $(d_{5R})^C$, and that in $\bar{u}$ is u_{5L} (the subscripts L and R mean the chirality). The corresponding scalar partners are denoted by the fields with tildes such as $\tilde{u}_{5L}$. The singlet expectation value V is assumed to be a bit larger than the electroweak scale ($V \gg v_u,\, v_d$) since the vector-like generations should be heavy to evade experimental bounds such as flavor constraints.

Hereafter, we call the present model including vector-like generations as the Vector-like Matter Supersymmetric Standard Model (VMSSM).

2.1 Gauge coupling unification

The VMSSM is quite different from the MSSM with respect to the RG running of coupling constants. In particular, the one-loop RG equations for gauge couplings are given by

$$\frac{dg_i}{d(\log \mu)} = b_i \frac{g_i^3}{16\pi^2}, \qquad (b_1, b_2, b_3) = \begin{cases} (\frac{33}{5}, 1, -3) & \text{(MSSM)} \\ (\frac{53}{5}, 5, 1) & \text{(VMSSM)} \end{cases} \tag{2.11}$$

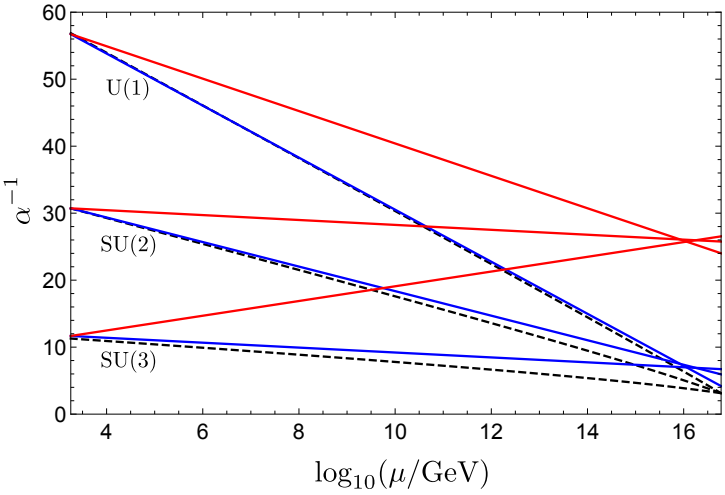

Figure 2.1: Gauge coupling unification in the MSSM (red) and the VMSSM (blue and dashed black). The red and blue lines are the one-loop RG running of $\alpha_i = g_i^2/4\pi$ $(i = 1, 2, 3)$ and the dashed ones are the two-loop running in the VMSSM. The horizontal axis denotes the renormalization scale μ.

where μ is renormalization scale and g_1, g_2 and g_3 are the gauge coupling constants of U(1), SU(2) and SU(3) gauge groups, respectively. In Fig. 2.1, we show the RG running of gauge coupling constants $\alpha_i = g_i^2/4\pi$ for the MSSM (red lines) and the VMSSM (blue ones). The two-loop RG running in the VMSSM is also shown by the dashed lines. The gauge coupling unification is kept in the VMSSM and the unified gauge coupling constant is defined as

$$\alpha_{\rm GUT} \;=\; \alpha_1(M_{\rm GUT}) = \alpha_2(M_{\rm GUT}) = \alpha_3(M_{\rm GUT}) \tag{2.12}$$

where the scale $M_{\rm GUT}$ of grand unified theory (GUT) is around 10^{16} GeV. In the figure, the unification scale in the VMSSM is found to be larger than the MSSM due to the two-loop RG effects of gauge couplings [14]. Further, the unified gauge coupling constant in the VMSSM becomes larger than the MSSM since the vector-like generations make the gauge couplings asymptotically non free. The large coupling constants in the gauge sector govern the low-energy behavior of other model parameters through the RG evolution. As will be seen later, this fact is important to analyze Yukawa and SUSY-breaking parameters. We use in the numerical calculation the two-loop RG equations for the gauge coupling constants and gaugino masses which are summarized in Appendix A.

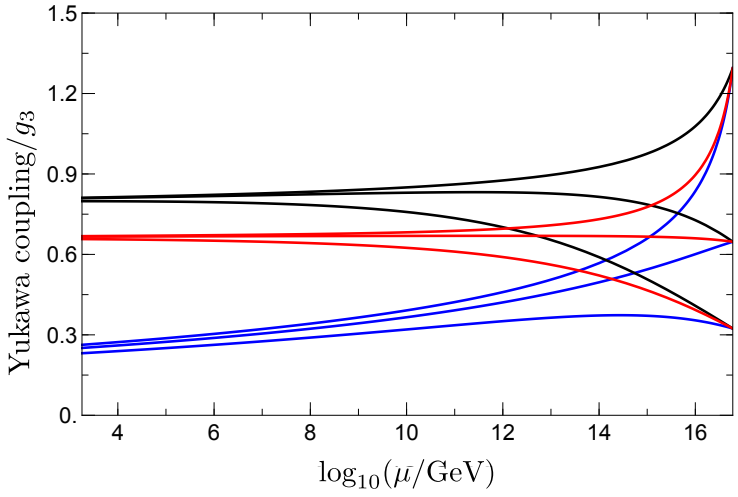

Figure 2.2: Typical RG flow of the 3rd generation Yukawa couplings $\boldsymbol{y}_{u_{33}}$ (black), $\boldsymbol{y}_{d_{33}}$ (red) and $\boldsymbol{y}_{e_{33}}$ (blue) normalized by g_3. The three lines for each Yukawa coupling correspond to the initial values 0.5, 1 and 2 from bottom to top. It is found that these Yukawa couplings have the strong convergence property in the infrared regime.

2.2 Yukawa couplings at the unification scale

In this subsection, we consider possible forms of the quark and lepton Yukawa couplings at the GUT scale. Due to the strong RG effect of gauge couplings, Yukawa couplings tend to have the fixed-point behavior at low energy [18]. Fig. 2.2 shows the typical RG flow of Yukawa couplings in case that $\boldsymbol{y}_{u_{33}}$, $\boldsymbol{y}_{d_{33}}$ and $\boldsymbol{y}_{e_{33}}$ are turned on. In the figure, all these couplings converge to their fixed-point values and are determined independently of their initial values at high energy.[1] By using this feature, it is possible to specify the matrix forms of Yukawa couplings for matter fields, that is, which elements can be non-vanishing at the GUT scale.

For the present purpose of calculating the Higgs boson mass and the muon $g-2$, it is sufficient to determine the Yukawa couplings except for the 1st generation. The matrix forms of Yukawa

[1]The predictions from infrared fixed points of RG equations are reliable only when the couplings indeed reach to their fixed points around the electroweak scale. Such strong convergence behavior can be realized [16] in asymptotically nonfree gauge theory (like the present VMSSM) and extra dimensional models, etc.

ϵ	$\hat{y}$	$\hat{Y}$	$\alpha_{\rm GUT}$	$M_{\rm GUT}$	$M_{\rm SUSY}$	V	$\tan\beta$
0.19	0.60	0.60	0.22	6.0×10^{16} GeV	1.8 TeV	4.0 TeV	17

Table 2.2: The set of input values.

couplings from the 2nd to 5th generations are given by

$$\text{up-type quarks} \quad : \quad \begin{array}{c} \\ 2 \\ 3 \\ 4 \\ 5 \end{array} \begin{array}{c} \begin{array}{cccc} 2 & 3 & 4 & 5 \end{array} \\ \begin{pmatrix} \epsilon^3\hat{y} & & \hat{y} & \epsilon^3\hat{Y} \\ & \hat{y} & & \\ \hat{y} & & & \hat{Y} \\ \epsilon^3\hat{Y} & & \hat{Y} & \hat{y} \end{pmatrix} \end{array}, \tag{2.13}$$

$$\text{down-type quarks} \quad : \quad \begin{array}{c} \\ 2 \\ 3 \\ 4 \\ 5 \end{array} \begin{array}{c} \begin{array}{cccc} 2 & 3 & 4 & 5 \end{array} \\ \begin{pmatrix} \epsilon^3\hat{y} & & \hat{y} & \epsilon^3\hat{Y} \\ & \epsilon\hat{y} & & \\ \hat{y} & & \hat{y} & \hat{Y} \\ \epsilon^3\hat{Y} & & \hat{Y} & \end{pmatrix} \end{array}, \tag{2.14}$$

$$\text{charged leptons} \quad : \quad \begin{array}{c} \\ 2 \\ 3 \\ 4 \\ 5 \end{array} \begin{array}{c} \begin{array}{cccc} 2 & 3 & 4 & 5 \end{array} \\ \begin{pmatrix} \epsilon^3\hat{y} & & 3\hat{y} & \epsilon^3\hat{Y} \\ & 3\epsilon\hat{y} & & \\ 3\hat{y} & & 3\hat{y} & \hat{Y} \\ \epsilon^3\hat{Y} & & \hat{Y} & \end{pmatrix} \end{array}, \tag{2.15}$$

where the blank entries mean 0, and each $\hat{y}$ ($\hat{Y}$) represents $\mathcal{O}(1)$ Yukawa coupling to the doublet (singlet) Higgs fields. The parameter ϵ is needed to reproduce the quark and lepton masses at low energy, especially for the 2nd generation [17]. In the charged-lepton matrix (2.15), the Georgi-Jarlskog factor [19] is utilized for the quark and lepton mass difference. We assume for simplicity that all $\hat{y}$ and $\hat{Y}$ in the matrices (2.13)–(2.15) are the same at the unification scale. With the input values listed in Table 2.2, we find the quark and lepton masses of 2nd and 3rd generations are properly reproduced at the weak scale. The scale $M_{\rm SUSY}$ is a typical threshold for supersymmetric particles, and the ratio of the vacuum expectation values of Higgs doublets is defined as $\tan\beta \equiv v_u/v_d$. In later sections, we will use these input values for the numerical analysis of the Higgs boson mass and the muon $g-2$.

There are two notable byproducts in the above forms of Yukawa matrices. First, in the matrix (2.13), the up-type Yukawa couplings of the 2-4 and 4-2 elements are $\mathcal{O}(1)$, that is, the vector-like generations strongly couple to the up-type Higgs field. This means that sizable radiative

corrections to the Higgs boson mass arise from these couplings in addition to the ordinary top Yukawa correction in the MSSM. Second, in the matrix (2.15), the 2-4 and 4-2 elements are $\mathcal{O}(1)$, that is, the vector-like generations strongly couple to the muon field. The radiative corrections from these couplings give the contribution to the muon $g-2$ in addition to the MSSM one. As mentioned in the introduction, the experimental data of the Higgs boson mass and the muon $g-2$ is difficult to be explained simultaneously in the MSSM. The new contributions from the strongly-coupled vector-like generations are expected to ameliorate the problem.

3 Analytic Formula

In this section, we present the analytic expressions for the one-loop radiative corrections to the Higgs boson mass and the muon $g-2$ in the VMSSM.

3.1 Higgs boson mass

The two Higgs doublets contain eight real scalar fields. Three of these are eaten to give masses to the gauge bosons and the remaining five are physical bosons; two charged scalars, one pseudoscalar, and two neutral scalars. Among them, it is well known in the MSSM that the tree-level mass of the lightest neutral scalar is below the Z boson mass. This lightest scalar mass is however raised up by including quantum corrections from the top and stop particles so that it becomes a plausible candidate for the 125 GeV Higgs boson found by the LHC experiments. We evaluate the mass of the lightest neutral scalar in the VMSSM, which is denoted by m_{h^0}, by calculating the scalar potential of the Higgs sector up to one-loop order. The quantum corrections to the Higgs mass from vector-like generations were calculated in the literature [20, 21]. We use the effective potential method [22] as usual for the MSSM case. The one-loop correction to the Higgs potential is generally given by

$$\Delta V_H = \sum_{X=u,d,e} \sum_{i=1}^{10} 2N_c \left[F(M^2_{\tilde{X}_i}) - F(M^2_{X_i}) \right], \qquad N_c = \begin{cases} 3 & (X = u, d) \\ 1 & (X = e) \end{cases} \tag{3.1}$$

where $M^2_{X_i}$ and $M^2_{\tilde{X}_i}$ are the squared-mass eigenvalues of fermions and scalars, respectively, which are obtained by diagonalizing (2.8)-(2.10) for fermions ($m_u^\dagger m_u$ and $m_u m_u^\dagger$, etc.) and (B.1)-(B.3) for scalars. The function F is defined as

$$F(x) = \frac{x^2}{64\pi^2} \left[\ln\left(\frac{x}{\mu^2}\right) - \frac{3}{2} \right], \tag{3.2}$$

where μ represents the renormalization scale which is set to be $M_{\rm SUSY}$ in evaluating the Higgs mass. The one-loop correction to the lightest neutral scalar mass, $\Delta m^2_{h^0}$, can be extracted from ΔV_H by

the formula [21]

$$\Delta m_{h^0}^2 = \left[\frac{\sin^2\beta}{2}\left(\frac{\partial^2}{\partial v_u^2} - \frac{1}{v_u}\frac{\partial}{\partial v_u}\right) + \frac{\cos^2\beta}{2}\left(\frac{\partial^2}{\partial v_d^2} - \frac{1}{v_d}\frac{\partial}{\partial v_d}\right) + \sin\beta\cos\beta\frac{\partial^2}{\partial v_u \partial v_d}\right]\Delta V_H. \tag{3.3}$$

3.2 Muon $g-2$

In order to evaluate the muon $g-2$, we use the mass eigenstate basis for gauginos, charged leptons, charged sleptons and neutral sleptons. First, we consider the 4×4 mass matrix for neutralinos consisting of bino ($\tilde{B}$), neutral wino ($\tilde{W}^0$) and neutral higgsinos ($\tilde{H}_u^0$ and $\tilde{H}_d^0$). In the basis of $\{\tilde{B}, \tilde{W}^0, \tilde{H}_d^0, \tilde{H}_u^0\}$, the neutralino mass matrix M_{χ^0} is given by

$$M_{\chi^0} = \begin{pmatrix} M_1 & 0 & -g_1 v_d/\sqrt{2} & g_1 v_u/\sqrt{2} \\ 0 & M_2 & g_2 v_d/\sqrt{2} & -g_2 v_u/\sqrt{2} \\ -g_1 v_d/\sqrt{2} & g_2 v_d/\sqrt{2} & 0 & -\mu_H \\ g_1 v_u/\sqrt{2} & -g_2 v_u/\sqrt{2} & -\mu_H & 0 \end{pmatrix}. \tag{3.4}$$

Next we consider the mass matrix for charginos consisting of charged winos ($\tilde{W}^\pm$) and charged higgsinos ($\tilde{H}_u^+$ and $\tilde{H}_d^-$), where the charged winos $\tilde{W}^\pm$ are defined as

$$\tilde{W}^\pm = \frac{i}{\sqrt{2}}(\tilde{W}^1 \mp i\tilde{W}^2). \tag{3.5}$$

In the basis of $\{\tilde{W}^-, \tilde{H}_d^-\}$ and $\{\tilde{W}^+, \tilde{H}_u^+\}$, the chargino mass matrix $M_{\chi^\pm}$ is given by

$$M_{\chi^\pm} = \begin{pmatrix} M_2 & \sqrt{2} g v_u \\ \sqrt{2} g v_d & \mu_H \end{pmatrix}. \tag{3.6}$$

These mass matrices are diagonalized as follows to obtain the muon interactions in terms of mass eigenstates. We first diagonalize the neutralino mass matrix (3.4) by using a unitary matrix N

$$N M_{\chi^0} N^\dagger = \mathrm{diag}\big(m_{\chi_1^0}, m_{\chi_2^0}, m_{\chi_3^0}, m_{\chi_4^0}\big), \tag{3.7}$$

where $m_{\chi_x^0}$ $(x = 1, \ldots, 4)$ are the positive mass eigenvalues, and $m_{\chi_x^0} < m_{\chi_y^0}$ if $x < y$. Similarly, the chargino mass matrix (3.6) is diagonalized by using two unitary matrices J and K

$$J M_{\chi^\pm} K^\dagger = \mathrm{diag}\big(m_{\chi_1^\pm}, m_{\chi_2^\pm}\big), \tag{3.8}$$

where $m_{\chi_x}^\pm$ $(x = 1, 2)$ are the positive mass eigenvalues, and $m_{\chi_1^\pm} < m_{\chi_2^\pm}$. Finally, we define the diagonalization of mass matrices for the lepton sector

$$(U_{e_R} m_e U_{e_L}^\dagger)_{ij} = m_{Ei}\delta_{ij} \quad (i, j = 1, \ldots, 5), \tag{3.9}$$

$$(U_{\tilde{e}} M_{\tilde{e}}^2 U_{\tilde{e}}^\dagger)_{ab} = m_{\tilde{E}_a}^2 \delta_{ab} \quad (a,b = 1,\ldots,10), \tag{3.10}$$

$$(U_{\tilde{\nu}} M_{\tilde{\nu}}^2 U_{\tilde{\nu}}^\dagger)_{\alpha\beta} = m_{\tilde{N}_\alpha}^2 \delta_{\alpha\beta} \quad (\alpha,\beta = 1,\ldots,5), \tag{3.11}$$

for charged leptons, charged sleptons and neutral sleptons, respectively. Here, m_e is the charged lepton mass matrix in Eq. (2.10), and $M_{\tilde{e}}^2$ and $M_{\tilde{\nu}}^2$ are the charged slepton and neutral slepton mass matrices in (B.3) and (B.4). Further we denote the mass eigenvalues m_{E_i}, $m_{\tilde{E}_a}$ and $m_{\tilde{N}_a}$ for the mass eigenstates of charged leptons (E_i), charged sleptons ($\tilde{E}_a$) and neutral sleptons ($\tilde{N}_\alpha$), respectively. With these diagonalized basis at hand, the interaction terms of the muon, which are needed to calculate the muon $g-2$, are given by

$$\begin{aligned}\mathcal{L} &= \sum_{a,x} \bar{E}_2 (n_{ax}^L P_L + n_{ax}^R P_R) \tilde{E}_a \chi_x^0 + \sum_{\alpha,x} \bar{E}_2 (c_{\alpha x}^L P_L + c_{\alpha x}^R P_R) \tilde{N}_\alpha \chi_x^\pm \\ &\quad + \sum_a \bar{E}_2 (s_a^L P_L + s_a^R P_R) \tilde{E}_a \chi_\Phi + \text{h.c.},\end{aligned} \tag{3.12}$$

where $P_L = (1-\gamma_5)/2$ and $P_R = (1+\gamma_5)/2$. The mass eigenstate E_2 corresponds to the muon field, and χ_x^0 and $\chi_x^\pm$ are the neutralinos and charginos. The fermion component of the singlet superfield Φ is denoted by χ_Φ and called the phino in this paper. The coefficients in the Lagrangian (3.12) are

$$\begin{aligned} n_{ax}^L = &- \sum_{i,j=1}^4 \boldsymbol{y}_{e_{ij}} (U_{e_R})_{i2} (U_{\tilde{e}})_{aj} N_{x3} + y_{\bar{e}} (U_{e_R})_{52} (U_{\tilde{e}})_{a,10} N_{x4} \\ &- \sum_{i=1}^4 \sqrt{2} g_1 (U_{e_R})_{i2} (U_{\tilde{e}})_{a,i+5} N_{x1} - \frac{g_2}{\sqrt{2}} (U_{e_R})_{52} (U_{\tilde{e}})_{a5} N_{x2} \\ &- \frac{g_1}{\sqrt{2}} (U_{e_R})_{52} (U_{\tilde{e}})_{a5} N_{x1}, \end{aligned} \tag{3.13}$$

$$\begin{aligned} n_{ax}^R = &\sum_{i,j=1}^4 \boldsymbol{y}_{e_{ij}} (U_{e_L})_{j2} (U_{\tilde{e}})_{a,i+5} N_{x3} - y_{\bar{e}} (U_{e_L})_{52} (U_{\tilde{e}})_{a5} N_{x4} \\ &+ \sum_{i=1}^4 \left[\frac{g_2}{\sqrt{2}} (U_{e_L})_{i2} (U_{\tilde{e}})_{ai} N_{x2} + \frac{g_1}{\sqrt{2}} (U_{e_L})_{i1} (U_{\tilde{e}})_{ai} N_{x1} \right] \\ &+ \sqrt{2} g_1 (U_{e_L})_{52} (U_{\tilde{e}})_{a,10} N_{x1}, \end{aligned} \tag{3.14}$$

$$c_{ax}^L = - \sum_{i,j=1}^4 \boldsymbol{y}_{e_{ij}} (U_{e_R})_{i2} (U_{\tilde{\nu}})_{aj} J_{x2} + g_2 (U_{e_R})_{52} (U_{\tilde{\nu}})_{a5} J_{x1}, \tag{3.15}$$

$$c_{ax}^R = y_{\bar{e}} (U_{e_L})_{52} (U_{\tilde{\nu}})_{a5} K_{x2} - \sum_{i=1}^4 g_2 (U_{e_L})_{i2} (U_{\tilde{\nu}})_{ai} K_{x1}, \tag{3.16}$$

$$s_a^L = \sum_{i=1}^4 \Big[- Y_{ei} (U_{e_R})_{i2} (U_{\tilde{e}})_{a,10} - Y_{Li} (U_{e_R})_{52} (U_{\tilde{e}})_{ai} \Big], \tag{3.17}$$

$$s_a^R = \sum_{i=1}^{4} \Big[- Y_{ei} (U_{e_L})_{52} (U_{\tilde{e}})_{a,i+5} - Y_{Li} (U_{e_L})_{i2} (U_{\tilde{e}})_{a5} \Big]. \tag{3.18}$$

In the VMSSM, the origins of SUSY contributions to the muon $g-2$ are divided into 3 parts [2] : neutralinos, charginos, and phino. The contribution from the phino is evaluated by the replacement χ^0 with χ_Φ in the neutralino diagram (with appropriate replacement of coefficients). We find the SUSY contribution to the muon $g-2$ in the VMSSM:

$$\Delta a_\mu^{\rm SUSY} = \Delta a_\mu^{\chi^0} + \Delta a_\mu^{\chi^\pm} + \Delta a_\mu^{\chi_\Phi}, \tag{3.19}$$

where

$$\Delta a_\mu^{\chi^0} = \sum_{a,x} \frac{1}{16\pi^2} \left[\frac{m_\mu m_{\chi_x^0}}{m^2_{\tilde{E}_a}} n^L_{ax} n^R_{ax} F_2^N(r_{1ax}) - \frac{m_\mu^2}{6 m^2_{\tilde{E}_a}} \big(n^L_{ax} n^L_{ax} + n^R_{ax} n^R_{ax} \big) F_1^N(r_{1ax}) \right], \tag{3.20}$$

$$\Delta a_\mu^{\chi^\pm} = \sum_{\alpha,x} \frac{1}{16\pi^2} \left[\frac{-3 m_\mu m^\pm_{\chi_x}}{m^2_{\tilde{\nu}_a}} c^L_{\alpha x} c^R_{\alpha x} F_2^C(r_{2\alpha x}) + \frac{m_\mu^2}{3 m^2_{\tilde{\nu}_\alpha}} \big(c^L_{\alpha x} c^L_{\alpha x} + c^R_{\alpha x} c^R_{\alpha x} \big) F_1^C(r_{2\alpha x}) \right], \tag{3.21}$$

$$\Delta a_\mu^{\chi_\Phi} = \sum_{a} \frac{1}{16\pi^2} \left[\frac{m_\mu m_{\chi_\Phi}}{m^2_{\tilde{E}_a}} s^L_a s^R_a F_2^N(r_{3a}) - \frac{m_\mu^2}{6 m^2_{\tilde{E}_a}} \big(s^L_a s^L_a + s^R_a s^R_a \big) F_1^N(r_{3a}) \right], \tag{3.22}$$

with $r_{1ax} = m^2_{\chi_x^0}/m^2_{\tilde{E}_a}$, $r_{2\alpha x} = m^2_{\chi_x^\pm}/m^2_{\tilde{N}_\alpha}$, $r_{3a} = m^2_{\chi_\Phi}/m^2_{\tilde{E}_a}$, and m_μ is the muon mass. The functions $F^N_{1,2}$ and $F^C_{1,2}$ are defined [10] by

$$F_1^N(x) = \frac{2}{(1-x)^4} \left(1 - 6x^2 + 3x^3 + 2x^3 - 6x^2 \ln x \right), \tag{3.23}$$

$$F_2^N(x) = \frac{3}{(1-x)^3} \left(1 - x^2 + 2x \ln x \right), \tag{3.24}$$

$$F_1^C(x) = \frac{2}{(1-x)^4} \left(2 + 3x - 6x^2 + x^3 + 6x \ln x \right), \tag{3.25}$$

$$F_2^C(x) = \frac{-3}{(1-x)^3} \left(3 - 4x + x^2 + 2 \ln x \right). \tag{3.26}$$

4 Numerical Result

In the following, we calculate the Higgs boson mass m_{h^0} and the correction to the muon $g-2$ by using the results (3.3) and (3.19).

[2] Strictly speaking, the non-SUSY contribution from the vector-like leptons, which is denoted by $\Delta a_\mu^{4+\bar{4}}$, has to be taken into account. That is, in the VMSSM the new physics contribution to the muon $g-2$ should be $\Delta a_\mu^{4+\bar{4}} + \Delta a_\mu^{\rm SUSY}$. However we numerically find $\Delta a_\mu^{4+\bar{4}}$ becomes $\mathcal{O}(10^{-12})$ by evaluating it in accordance with Ref. [23], and drop it in the following analysis.

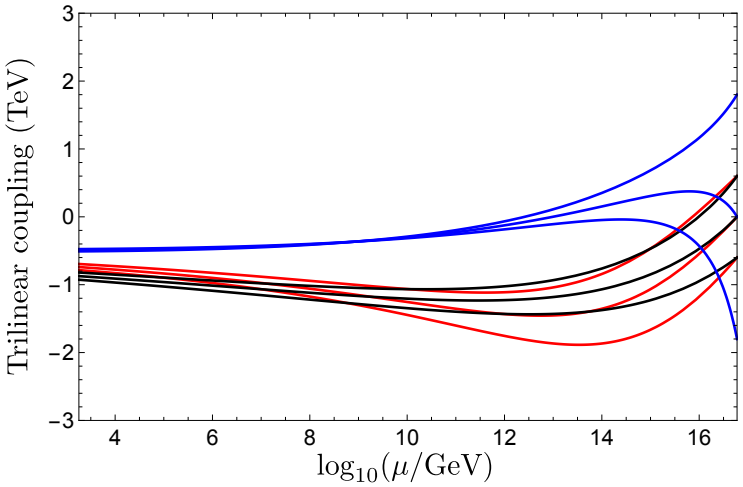

Figure 4.1: Typical RG flow of the scalar trilinear couplings $\boldsymbol{a}_{u_{33}}$ (red), $a_{\bar{u}}$ (black) and $\boldsymbol{a}_{e_{24}}$ (blue). The three lines for each coupling correspond to the initial values $A_0 = -1.0$, 0, 1.0 TeV from bottom to top. It is found that these trilinear couplings have the strong convergence property in the infrared regime.

4.1 SUSY-breaking parameters

As for the SUSY breaking scenario, we use the minimal gravity mediation [24] which leads to the superpartner spectrum by assuming that all gaugino masses unify to $m_{1/2}$ and all scalar soft masses also unify to m_0 at the GUT scale. The other relevant SUSY-breaking parameters is A_0, which is the universal scalar trilinear coupling at the GUT scale. In this paper, $\tan\beta$ is fixed so that the experimental data of the muon mass is obtained at the electroweak scale for fixed values of Yukawa couplings. Furthermore, the sign of μ_H parameter is taken to be positive for the muon $g-2$ anomaly. As a result, in the following analysis we have three SUSY-breaking free parameters: $m_{1/2}$, m_0 and A_0. Once these parameters are fixed together with the input values listed in Table 2.2, the resultant low-energy physics is determined by solving the RG equations.

We here comment on typical property of scalar trilinear couplings in the VMSSM. Fig. 4.1 shows the RG running of several trilinear couplings which are relevant to the Higgs boson mass and the muon $g-2$. The red and black lines mean the energy dependence of $\boldsymbol{a}_{u_{33}}$ and $a_{\bar{u}}$ which would give sizable radiative corrections to the Higgs boson mass. The blue lines show the energy dependence of $\boldsymbol{a}_{e_{24}}$ which would contribute to the muon $g-2$. It is found that these trilinear couplings have the strong infrared convergency as in the case of Yukawa couplings described in Fig. 2.2.

In the MSSM, it is known that the mass of the lightest neutral scalar depends on the trilinear

coupling of stop [5]. In the VMSSM, taking into account the infrared convergence behavior, one expects that the Higgs boson mass does not depend on the initial values of trilinear couplings at high energy. Moreover, one might also consider that the same is true for the muon $g-2$. We will however show that the muon $g-2$ depend on the universal trilinear coupling A_0 in particular circumstance, and discuss the reason in detail in Section 4.3.

4.2 Parameter dependence of Higgs boson mass

We first study the dependence of the Higgs boson mass m_{h^0} on the SUSY-breaking parameters and the stop mass. We also compare the contribution from the vector-like generations with that from the MSSM sector. Figs. 4.2 show our m_{h^0} results in various situations. The orange regions in these figures reproduce the Higgs boson mass between 124.7 and 126.2 GeV. First, the upper left panel shows the dependence on the universal gaugino mass $m_{1/2}$, where the universal trilinear coupling A_0 is set to 0 GeV. The three black lines correspond to the universal scalar soft mass $m_0 = 250$, 500, 1000 GeV from bottom to top. As seen from this panel, the Higgs boson becomes heavier when $m_{1/2}$ is larger. This is originated from the RG property that low-energy squark masses become large when $m_{1/2}$ is set to be large. It is also noted that m_{h^0} becomes large as m_0 increases. In the upper right panel, we show the A_0 dependence of m_{h^0}, assuming $m_{1/2} = 2150$ GeV and $m_0 = 250$, 500, 1000 GeV from bottom to top. As discussed in the previous subsection, the Higgs boson mass does not depend on A_0 due to the infrared convergence RG behavior of trilinear couplings.

In the lower left panel, we show the dependence of m_{h^0} on the stop mass which is denoted by $m_{\tilde{u}_{3L}}$. The orange region is explained if the stop mass is from 2.0 to 2.2 TeV. In the MSSM the stop mass is needed to be $3-4$ TeV to explain the Higgs mass around 125 GeV [25]. In the VMSSM, however, m_{h^0} is explained by a lighter stop than the MSSM. That is clearly seen in the lower right panel which shows the Higgs boson mass including the radiative corrections from the VMSSM (red line) and from the MSSM sector only (black line) with m_0 and A_0 being 250 and 0 GeV, respectively. The black line is defined by taking the limit of large V which means the decoupling of vector-like generations. In the VMSSM, the Higgs boson mass turns out to be explained by a smaller value of $m_{1/2}$, that is, lighter low-energy squarks than the MSSM. This is because there exists additional radiative corrections from the vector-like generations which have sizable coupling to the Higgs fields.

4.3 Parameter dependence of muon $g-2$

Next we study the parameter dependences of the SUSY contribution $\Delta a_\mu^{\rm SUSY}$ on the SUSY-breaking parameters and the smuon mass. We also compare the contribution from the vector-like generations with that from the MSSM sector. Figs. 4.3 show our $\Delta a_\mu^{\rm SUSY}$ results in various situations. The blue regions explain the muon $g-2$ anomaly within the 1σ level. First, the upper left panel of

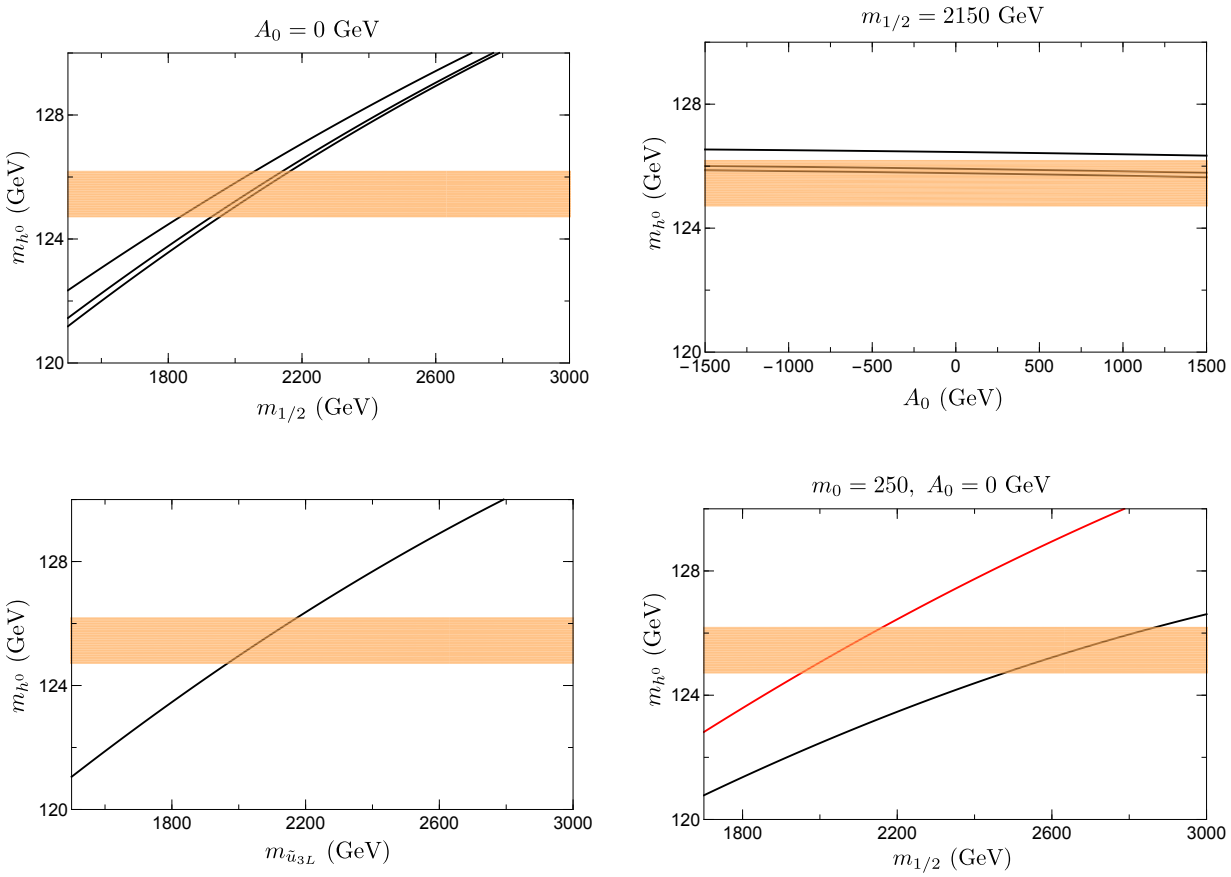

Figure 4.2: The dependence of the lightest Higgs mass m_{h^0} on $m_{1/2}$ (upper left), A_0 (upper right), and the stop mass (lower left). The lower right panel shows m_{h^0} including the radiative corrections in the VMSSM (red) and in the MSSM (black) with $m_0 = 250$ and $A_0 = 0$ GeV. The orange regions represent the Higgs boson with a mass between 124.7 and 126.2 GeV. In the upper left panel, the three lines are $m_0 = 250$, 500, 1000 GeV from bottom to top, and A_0 is fixed to 0 GeV. In the upper right panel, the three lines are $m_0 = 250$, 500, 1000 GeV from bottom to top, and $m_{1/2}$ is fixed to 2150 GeV.

Fig. 4.3 shows the dependence on the universal gaugino mass $m_{1/2}$, where the universal trilinear coupling A_0 is set to 0 GeV. The three black lines correspond to $m_0 = 250$, 500, 1000 GeV from top to bottom. As seen from this panel, the $g-2$ contribution $\Delta a_\mu^{\rm SUSY}$ becomes smaller when $m_{1/2}$ and m_0 are larger. This is originated from the decoupling property in Eqs. (3.20)-(3.22) that the SUSY contribution becomes small when the superpartners become heavy. In the upper right panel, we show the A_0 dependence of $\Delta a_\mu^{\rm SUSY}$, assuming $m_{1/2} = 2150$ GeV, $m_0 = 250$, 500, 1000 GeV from top to bottom. An interesting A_0 dependence is found in this panel: When scalar soft masses are small (e.g. $m_0 = 250$ and 500 GeV in the panel), the $g-2$ contribution becomes larger as A_0 increases. On the other hand, if scalar soft masses are large ($m_0 = 1000$ GeV in the panel), the $g-2$ contribution is almost insensitive to A_0. This behavior is understood in a following way. In the charged slepton mass matrix (B.14), the off-diagonal mixing from the 1st to 4th generations are given by $\boldsymbol{a}_{e_{ij}} v_d - \mu_H^* \boldsymbol{y}_{e_{ij}} v_u$ where the second term is dominant with large $\tan\beta$ and the first A-parameter-dependent term is ignored. On the other hand, the off-diagonal mixing with the 5th generation takes the form $A_{e_i} V + Y_{e_i} Y^* |V|^2$ where both terms are similar order. If m_0 is small, the mixing with the 5th generation becomes nearly comparable with the diagonal part at low energy, and one of the pair of vector-like particles becomes light after the diagonalization.

In the lower left panel, we show the dependence on the smuon mass which is denoted by $m_{\tilde{e}_{2L}}$. The blue region is explained if the smuon mass is around 1 TeV. In the MSSM that the smuon mass is needed to be $\mathcal{O}(100)$ GeV to explain the anomaly. In the VMSSM, however, the deviation of the muon $g-2$ is explained by a heavier smuon than the MSSM. This is clearly seen in the lower right panel which shows the muon $g-2$ contribution from the VMSSM (red line) and from the MSSM sector only (black line). The definition of the black line is the large V limit and the same as before. In the VMSSM, the muon $g-2$ anomaly turns out to be explained by a larger value of $m_{1/2}$, that is, a heavier low-energy smuon than the MSSM. This is because there exists additional contribution from the vector-like generations which have sizable coupling to the muon field.

We also show in Fig. 4.4 each $g-2$ contribution from SUSY particles. The blue and green lines represent the contributions from neutralinos and charginos, respectively. The phino contribution is negligible ($\Delta a_\mu^{\chi\Phi} \sim 10^{-11}$) in this figure mainly because the gauge couplings are absent in (3.17) and (3.18). In the VMSSM with the parameter set of Table 2.2, it is found that the neutralino contribution tends to be dominant than the chargino one. It comes from the superpartner spectrum that a charged slepton of $\mathcal{O}(100)$ GeV exists, while the neutral sleptons are $\mathcal{O}(1)$ TeV. The concrete mass spectrum are listed in the next section.

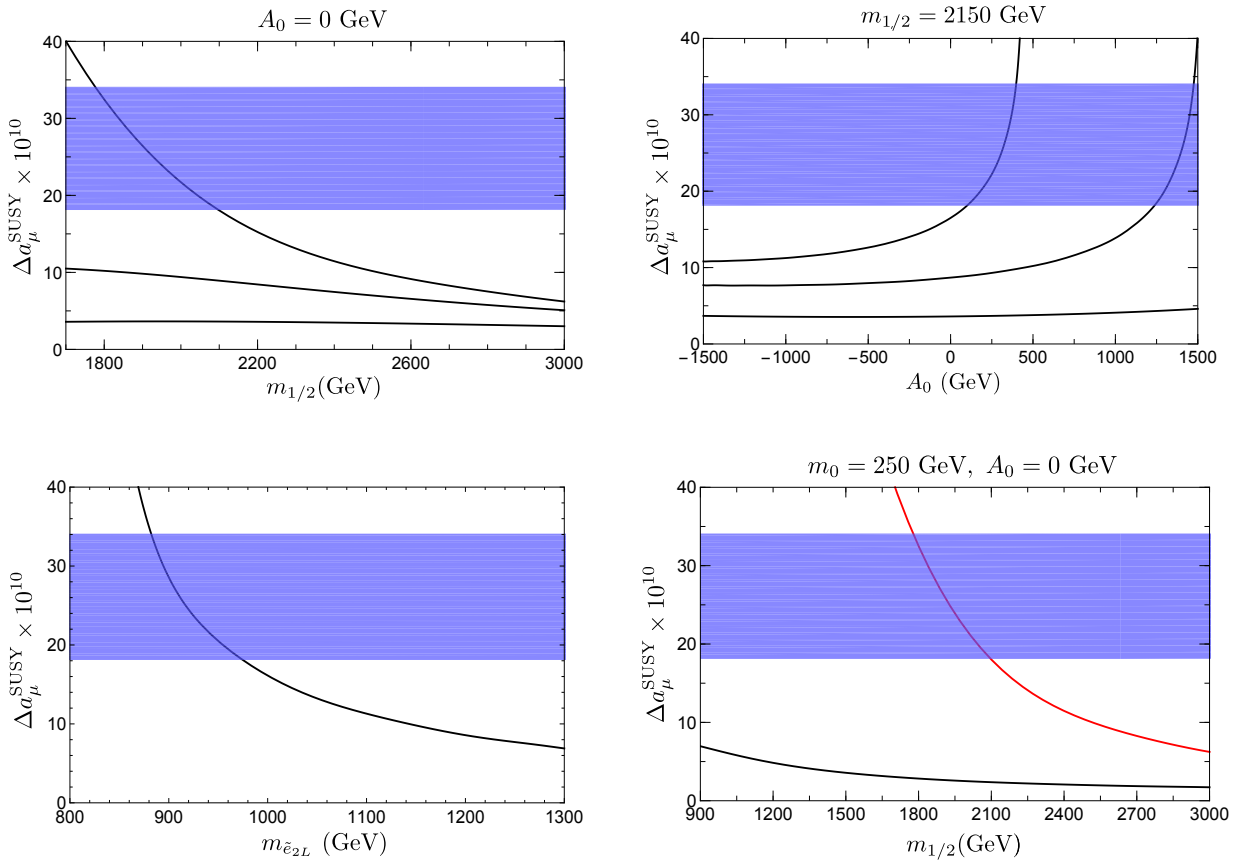

Figure 4.3: The dependence of the muon $g-2$ contribution $\Delta a_\mu^{\rm SUSY}$ on $m_{1/2}$ (upper left), A_0 (upper right) and the smuon mass (lower left). The lower right panel shows the muon $g-2$ in the VMSSM (red) and in the MSSM (black) with $m_0 = 250$ and $A_0 = 0$ GeV. The blue regions explains the deviation between the SM prediction and the experimental result within 1σ. In the upper left panel, the three lines are $m_0 = 250$, 500, 1000 GeV from top to bottom, and A_0 is fixed to 0 GeV. In the upper right panel, the three lines are $m_0 = 250$, 500, 1000 GeV from top to bottom, and $m_{1/2}$ is fixed to 2150 GeV.

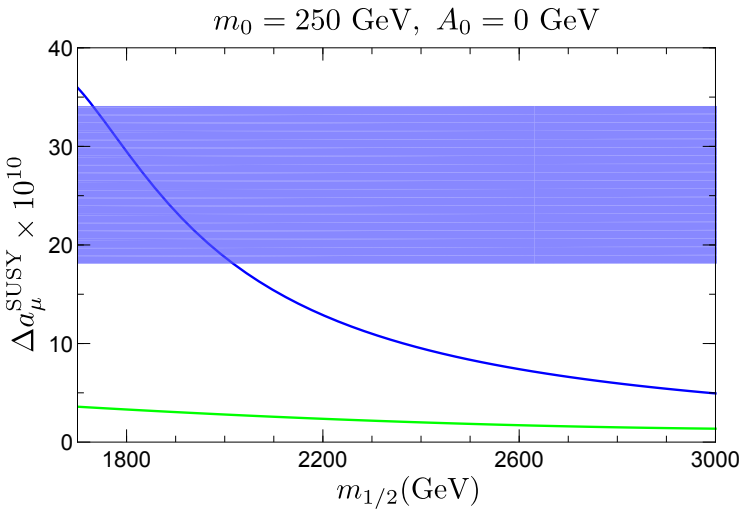

Figure 4.4: The blue and green lines represent the muon $g-2$ contributions from neutralinos and charginos, respectively. The blue regions explains the deviation between the SM prediction and the experimental result within 1σ.

4.4 Higgs boson mass and muon $g-2$ in the VMSSM

Before estimating the Higgs boson mass and the muon $g-2$, we comment on the experimental bounds about the masses of vector-like generations and superparticles. For the fermion masses of vector-like generations, the experimental lower bounds of quarks and charged leptons are roughly given by 700 GeV and 100 GeV, respectively [26]. In the VMSSM, the 4-5 and 5-4 components of Yukawa couplings in (2.13)-(2.15) are $\mathcal{O}(1)$ and the expectation value V is set to 4000 GeV. Thus the quarks and leptons of vector-like generations respectively become $\mathcal{O}(1)$ TeV and about 200 GeV, which satisfy the experimental bounds.

The gaugino, especially the gluino gives an important experimental bound on the superpartner mass spectrum. This is because in the VMSSM the gauge couplings are asymptotically non free and the universal gaugino mass is much larger than low-energy gaugino masses. The low-energy values of gaugino mass parameters are shown in Fig. 4.5 where the horizontal dashed line means 800 GeV, a rough lower experimental bound of gluino mass [26]. It is found that the universal gaugino mass $m_{1/2}$ should be taken above 1.9 TeV. The squarks of first two generations are roughly excluded with masses below 1100 GeV, and the superpartners of the top and bottom quarks should be heavier than 95 GeV and 89 GeV, respectively [26]. The lower left panel of Fig. 4.2 implies that the stop mass in the VMSSM is about 2 TeV for the Higgs boson mass being around 125 GeV. Since the RG evolution of squark mass parameters is governed by the strong gauge coupling, the other squark

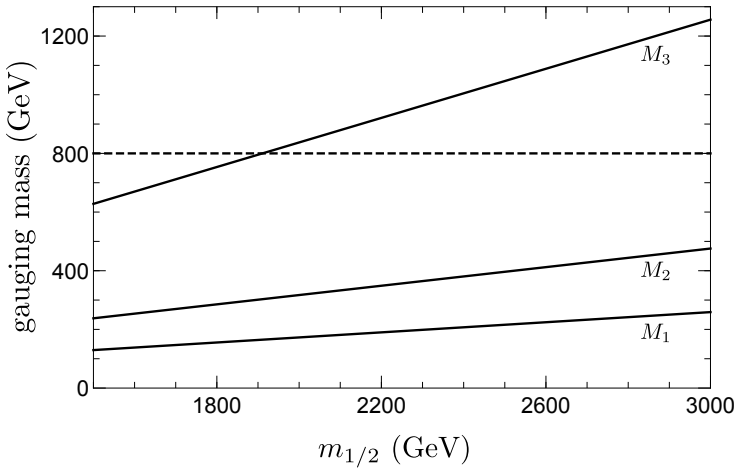

Figure 4.5: The mass parameters of bino (M_1), wino (M_2) and gluino (M_3) at $M_{\rm SUSY}$ for the universal gaugino mass $m_{1/2}$ at $M_{\rm GUT}$. The dashed line (800 GeV) represents a rough experimental lower bound of the gluino mass.

masses are of the same order of the stop mass. Thus the parameter regions appropriate for the Higgs boson mass and the muon $g-2$ are allowed by the squark mass bounds in the VMSSM. For the charged and neutral sleptons, the experimental mass bound is roughly given by 80 GeV [26]. As seen from Fig. 4.3, the muon $g-2$ anomaly is explained if the smuon mass is $\mathcal{O}(1)$ TeV. The other soft mass parameters for sleptons have similar RG behaviors as the smuon and hence all sleptons, except for the charged sleptons of vector-like generations, are $\mathcal{O}(1)$ TeV at low energy which satisfy the experimental mass bound. As mentioned previously, one of the charged sleptons of vector-like generations becomes $\mathcal{O}(100)$ GeV when the universal gaugino mass $m_{1/2}$ and/or soft scalar mass m_0 are small. We take into account this slepton mass bound as well as the above gluon mass bound in the following analysis.

In Fig. 4.6, we plot the contours of the Higgs boson mass and the muon $g-2$ in the $m_{1/2}$–m_0 plane. The other mass parameter A_0 is fixed to 0 GeV (left panel) and 1000 GeV (right panel). The orange region of parameters reproduces the Higgs boson mass from 124.7 to 126.2 GeV. The blue and green regions explain the muon $g-2$ anomaly within the 1σ and 2σ level, respectively. The black and gray regions are excluded by the experimental mass bounds of the gluino and the charged sleptons of vector-like generations, respectively. It is found from the comparison between $A_0 = 0$ and $A_0 = 1000$ GeV that the muon $g-2$ is sensitive to A_0 whereas the Higgs boson mass is not. This is the parameter dependence mentioned in Subsections 4.2 and 4.3.

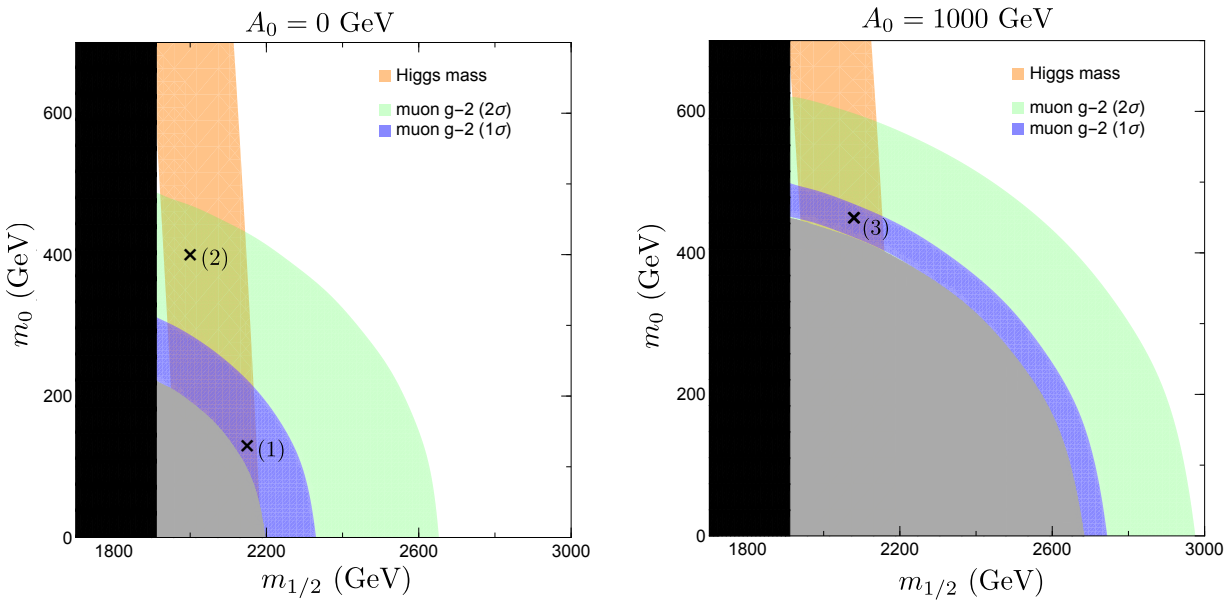

Figure 4.6: The Higgs boson mass and the muon $g-2$ anomaly in the VMSSM. The universal trilinear coupling A_0 is set to 0 (left) and 1000 GeV (right). The orange region reproduces the Higgs boson mass, and the blue and green regions explain the muon $g-2$ anomaly. The black and gray regions are excluded by the mass bounds of the gluino and the charged sleptons of vector-like generations. See the text for details. The cross marks (1)-(3) in the figures are the sample points whose mass parameters and spectrum are summarized in Table 4.1.

	Point (1)	Point (2)	Point (3)
$m_{1/2}$	2150	2000	2080
m_0	130	400	450
A_0	0	0	1000
M_3	900.0	837.1	864
$m_{\chi_1^0}$	185.5	172.6	177.6
$m_{\chi_1^\pm}$	340.8	317. 1	325.9
$m_{\tilde{u}_{3L}}$, $m_{\tilde{u}_{3H}}$	1926, 2433	1811, 2385	1898, 2383
$m_{\tilde{u}_{4L,4H,5L,5H}}$	$2715 - 3973$	$2641 - 3874$	$2691 - 3926$
$m_{\tilde{e}_{2L}}$, $m_{\tilde{e}_{2H}}$	952.2, 1221	922.4, 1181	921.3, 1220
$m_{\tilde{e}_{4L}}$	107.4	302.5	150.5
$m_{\tilde{e}_{4H,5L,5H}}$	$1129 - 1860$	$1112 - 1808$	$1119 - 1862$
$m_{\tilde{\nu}_2}$	1227	1186	1223
$m_{\tilde{\nu}_{4,5}}$	816, 1773	821, 1718	815, 1771
m_{h^0}	126.0	125.1	125.6
$\Delta a_\mu^{\rm SUSY}$	26.1×10^{-10}	12.1×10^{-10}	21.1×10^{-10}

Table 4.1: The sample points in the VMSSM. All the mass parameters are given in unit of GeV.

We discuss how the vector-like generations contribute to the Higgs boson mass and the muon $g-2$ by comparing the VMSSM results with the MSSM. Several patterns of model parameters and mass spectrum are listed in Table 4.1. We choose three benchmark points which simultaneously explain the Higgs boson mass and the muon $g-2$ anomaly: $(m_{1/2}, m_0, A_0) = (2150, 130, 0)$, $(2000, 400, 0)$, $(2080, 450, 1000)$ as Point (1), (2), (3), respectively. These points are marked by (1)-(3) in Fig. 4.6. We show in the table the mass eigenvalues of scalar superpartners which are related to the quantum corrections to the Higgs boson mass and the muon $g-2$: the stop ($m_{\tilde{u}_{3L,3H}}$), the smuon ($m_{\tilde{e}_{2L,2H}}$), the sneutrino of 2nd generation ($m_{\tilde{\nu}_2}$), the vector-like up-type squarks ($m_{\tilde{u}_{4L,4H,5L,5H}}$), the vector-like charged sleptons ($m_{\tilde{e}_{4L,4H,5L,5H}}$), and the vector-like neutral sleptons ($m_{\tilde{\nu}_{4,5}}$). The labels L and H of the stop and smuon mean that L is lighter than H. For the vector-like generations, the mass eigenvalues are arranged to be heavy in the order of 4L, 4H, 5L, 5H for squarks and charged sleptons, and 4, 5 for neutral sleptons. In the MSSM, the stop masses are roughly needed to be $3-4$ TeV for the Higgs mass, though it depends on other parameters. In the VMSSM with the universal SUSY-breaking parameters, the Higgs mass is reproduced by lighter stop masses. This is because we have extra up-type (s)quarks that strongly couple to the Higgs fields, namely the Yukawa couplings of vector-like quarks remains $\mathcal{O}(1)$ at low energy. That gives an additional quantum correction to the Higgs boson mass and relaxes the requirement of large stop masses in the MSSM. As for the muon

$g-2$, the anomaly can be explained by 1 TeV smuon masses in the VMSSM. In this paper, we fix $\tan\beta = 17$ to obtain the quark and lepton masses in the 2nd and 3rd generations. If the muon $g-2$ is evaluated with $\tan\beta = 17$ in the MSSM, the smuon masses are needed to be light and $\mathcal{O}(100)$ GeV to explain the deviation [9, 10]. In the VMSSM, one of the charged sleptons in the vector-like generations, $m_{\tilde{e}_{4L}}$ in Table 4.1, becomes $\mathcal{O}(100)$ GeV. Moreover the Yukawa couplings between the 2nd and vector-like generations, the 2-4 and 4-2 elements in (2.15), are nonzero. These facts together mean that the muon couplings (3.13)-(3.16) give sizable $g-2$ contributions from extra generations. In the end, the deviation between the SM theoretical values and the experimental measurement can be explained even if the smuon masses are much heavier than the MSSM.

Finally we comment on the flavor constraints in the VMSSM. Notice that the following is a tentative analysis which depends on how to realize the generation mixing including (the Yukawa couplings of) the first generation. A typical experimental bound in the quark sector comes from the unitarity of the generation mixing matrix, which is numerically confirmed to be satisfied with heavy vector-like generations. In the lepton sector, the muon has sizable couplings to the vector-like generations, which would induce flavor-changing rare processes.[3] The flavor mixing including the third generation (τ) is expected to be small since μ-τ has no coupling in (2.15) and is only radiatively induced. On the other hand, the muon decay, especially $\mu \to e\gamma$, would be induced through the slepton mixing which is represented by the product of couplings among the first two generations and vector-like ones. A previous analysis shows the branching ratio of $\mu \to e\gamma$ becomes $\mathcal{O}(10^{-13})$ which is almost the same order of the experimental bound [28], when the above product of couplings is $\mathcal{O}(10^{-1})$ [29]. In the present model, the muon coupling to the vector-like generations is found to be $\mathcal{O}(10^{-1})$ at low energy and that of the electron is expected to be smaller. Thus, within the region where the Higgs boson mass and the muon $g-2$ are explained simultaneously, the $\mu \to e\gamma$ decay would not be comparable with the experimental bound.

5 Conclusion

In this paper, we have studied the Higgs boson mass and the muon $g-2$ anomaly in an extension of the MSSM by introducing one pair of vector-like generations. Compared with the MSSM, the Higgs mass is reproduced with a lighter stop, while the muon $g-2$ is fitted by a heavier smuon. As a result, we found that these two experimental values can be explained simultaneously in wide regions of SUSY-breaking parameter space. The model parameters are controlled by the strong gauge coupling (and the gluino mass) through the infrared convergence of RG evolution. Due to this feature, the quark and lepton Yukawa couplings at high energy and the SUSY mass spectrum

[3] For the neutrino physics with low-scale vector-like generations, see [27] for example.

at low energy are highly restricted, which leads to distinctive physical predictions. Among them, the gluino mass becomes around 900 GeV and the lightest neutralino and chargino are $\mathcal{O}(100)$ GeV with the Higgs mass and the muon $g-2$ being realized. These mass regions would be measurable in near future experiments.

We comment on the phenomenology of the singlet superfield Φ, whose fermionic component is called the phino in this paper. The phino mass read from the superpotential and is given by YV where Y is the coefficient of the cubic term of gauge singlet Φ. The RG running of Y is governed only by the Yukawa couplings involving Φ and does not contains any gauge couplings, which mean Y is pushed down during the RG evolution. As a result, Y becomes $\mathcal{O}(10^{-2})$ at low energy and the mass of phino is around or below 100 GeV. Since the lightest neutralino is around 200 GeV (see Table 4.1), the phino may be the lightest superparticle, which implies the neutral and non-baryonic phino can be a reasonable candidate for the dark matter in the universe and may also give characteristic collider signatures. That should be investigated in detail, together with the phenomenology of the scalar component of Φ, e.g., a recent analysis of the 750 GeV diphoton excess [30] with Φ and vector-like generations [31].

Acknowledgments

The authors thank Tetsutaro Higaki, Naoki Yamamoto, Ryo Yokokura for useful discussions and comments. This work was supported in part by KLL PhD Program Research Grant from Keio University.

A RG Equations for the VMSSM

We present the RG equations of model parameters in the VMSSM. Due to the asymptotically non-free nature of the gauge sector, the two-loop RG equations are used for gauge coupling constants and gaugino masses.

A.1 Gauge couplings and gaugino masses

The two-loop RG equations of gauge coupling constants g_i and gaugino masses M_i $(i = 1, 2, 3)$ are given by

$$\frac{dg_i}{d(\log\mu)} = b_i\frac{g_i^3}{16\pi^2} + \frac{g_i^3}{(16\pi^2)^2}\Bigg[\sum_j b_{ij}g_j^2 - \sum_{a=u,d,e} c_{ia}\Big[\mathrm{Tr}\big(\boldsymbol{y}_a^\dagger\boldsymbol{y}_a\big) + y_{\bar{a}}^* y_{\bar{a}}\Big] - \sum_{k=1}^{4}\sum_{x=Q,u,d,L,e} d_{ix}Y_{x_k}^* Y_{x_k}\Bigg], \tag{A.1}$$

$$\frac{dM_i}{d(\log\mu)} = 2b_i\frac{g_i^2 M_i}{16\pi^2} + \frac{2g_i^2}{(16\pi^2)^2}\Bigg[\sum_j b_{ij}g_j^2(M_i + M_j) + \sum_{a=u,d,e} c_{ia}\Big[\mathrm{Tr}\big(\boldsymbol{y}_a^\dagger\boldsymbol{a}_a\big) + y_{\bar{a}}^* a_{\bar{a}} - M_i\big[\mathrm{Tr}(\boldsymbol{y}_a^\dagger\boldsymbol{y}_a) + y_{\bar{a}}^* y_{\bar{a}}\big]\Big] + \sum_{k=1}^{4}\sum_{x=Q,u,d,L,e} d_{ix}(Y_{x_k}^* A_{x_k} - M_i Y_{x_k}^* Y_{x_k})\Bigg], \tag{A.2}$$

where the one-loop beta function coefficients are $b_i = (53/5, 5, 1)$, and the coefficient matrices b_{ij}, c_{ia}, d_{ix} are

$$b_{ij} = \begin{pmatrix} 977/75 & 39/5 & 88/3 \\ 13/5 & 53 & 40 \\ 11/3 & 15 & 178/3 \end{pmatrix}, \tag{A.3}$$

$$c_{ia} = \begin{array}{c} \begin{matrix} u & d & e \end{matrix} \\ \begin{pmatrix} 26/5 & 14/5 & 18/5 \\ 6 & 6 & 2 \\ 4 & 4 & 0 \end{pmatrix} \end{array}, \tag{A.4}$$

$$d_{ix} = \begin{array}{c} \begin{matrix} Q & u & d & L & e \end{matrix} \\ \begin{pmatrix} 2/5 & 16/5 & 4/5 & 6/5 & 12/5 \\ 6 & 0 & 0 & 2 & 0 \\ 4 & 2 & 2 & 0 & 0 \end{pmatrix} \end{array}. \tag{A.5}$$

A.2 Yukawa couplings and bilinear terms

The RG equations of Yukawa couplings and the bilinear terms are given by

$$\frac{d\boldsymbol{y}_{u_{ij}}}{d(\log\mu)} = (\gamma_u\boldsymbol{y}_u)_{ij} + (\boldsymbol{y}_u\gamma_Q)_{ij} + \gamma_{H_u}\boldsymbol{y}_{u_{ij}}, \tag{A.6}$$

$$\frac{d\boldsymbol{y}_{d_{ij}}}{d(\log\mu)} = (\gamma_d \boldsymbol{y}_d)_{ij} + (\boldsymbol{y}_d \gamma_Q)_{ij} + \gamma_{H_d} \boldsymbol{y}_{d_{ij}}, \tag{A.7}$$

$$\frac{d\boldsymbol{y}_{e_{ij}}}{d(\log\mu)} = (\gamma_e \boldsymbol{y}_e)_{ij} + (\boldsymbol{y}_e \gamma_L)_{ij} + \gamma_{H_d} \boldsymbol{y}_{e_{ij}}, \tag{A.8}$$

$$\frac{dy_{\bar{u}}}{d(\log\mu)} = (\gamma_{\bar{u}} + \gamma_{\bar{Q}} + \gamma_{H_d}) y_{\bar{u}}, \tag{A.9}$$

$$\frac{dy_{\bar{d}}}{d(\log\mu)} = (\gamma_{\bar{d}} + \gamma_{\bar{Q}} + \gamma_{H_u}) y_{\bar{d}}, \tag{A.10}$$

$$\frac{dy_{\bar{e}}}{d(\log\mu)} = (\gamma_{\bar{e}} + \gamma_{\bar{L}} + \gamma_{H_u}) y_{\bar{e}}, \tag{A.11}$$

$$\frac{dY_{Q_i}}{d(\log\mu)} = (Y_Q \gamma_Q)_i + (\gamma_{\bar{Q}} + \gamma_\Phi) Y_{Q_i}, \tag{A.12}$$

$$\frac{dY_{u_i}}{d(\log\mu)} = (\gamma_u Y_u)_i + (\gamma_{\bar{u}} + \gamma_\Phi) Y_{u_i}, \tag{A.13}$$

$$\frac{dY_{d_i}}{d(\log\mu)} = (\gamma_d Y_d)_i + (\gamma_{\bar{d}} + \gamma_\Phi) Y_{d_i}, \tag{A.14}$$

$$\frac{dY_{L_i}}{d(\log\mu)} = (Y_L \gamma_L)_i + (\gamma_{\bar{L}} + \gamma_\Phi) Y_{L_i}, \tag{A.15}$$

$$\frac{dY_{e_i}}{d(\log\mu)} = (\gamma_e Y_e)_i + (\gamma_{\bar{e}} + \gamma_\Phi) Y_{e_i}, \tag{A.16}$$

$$\frac{dY}{d(\log\mu)} = 3\gamma_\Phi Y, \tag{A.17}$$

$$\frac{d\mu_H}{d(\log\mu)} = (\gamma_{H_u} + \gamma_{H_d}) \mu_H, \tag{A.18}$$

$$\frac{dM}{d(\log\mu)} = 2\gamma_\Phi M. \tag{A.19}$$

The anomalous dimensions γ's are

$$\gamma_{Q_{ij}} = \frac{1}{16\pi^2}\left[\left(\boldsymbol{y}_u^\dagger \boldsymbol{y}_u + \boldsymbol{y}_d^\dagger \boldsymbol{y}_d\right)_{ij} + Y_{Q_i}^* Y_{Q_j} - \left(\frac{8}{3}g_3^2 + \frac{3}{2}g_2^2 + \frac{1}{30}g_1^2\right)\delta_{ij}\right], \tag{A.20}$$

$$\gamma_{u_{ij}} = \frac{1}{16\pi^2}\left[2\left(\boldsymbol{y}_u \boldsymbol{y}_u^\dagger\right)_{ij} + Y_{u_i} Y_{u_j}^* - \left(\frac{8}{3}g_3^2 + \frac{8}{15}g_1^2\right)\delta_{ij}\right], \tag{A.21}$$

$$\gamma_{d_{ij}} = \frac{1}{16\pi^2}\left[2\left(\boldsymbol{y}_d \boldsymbol{y}_d^\dagger\right)_{ij} + Y_{d_i} Y_{d_j}^* - \left(\frac{8}{3}g_3^2 + \frac{2}{15}g_1^2\right)\delta_{ij}\right], \tag{A.22}$$

$$\gamma_{L_{ij}} = \frac{1}{16\pi^2}\left[\left(\boldsymbol{y}_e^\dagger \boldsymbol{y}_e\right)_{ij} + Y_{L_i}^* Y_{L_j} - \left(\frac{3}{2}g_2^2 + \frac{3}{10}g_1^2\right)\delta_{ij}\right], \tag{A.23}$$

$$\gamma_{e_{ij}} = \frac{1}{16\pi^2}\left[2\left(\boldsymbol{y}_e^\dagger \boldsymbol{y}_e\right)_{ij} + Y_{e_i} Y_{e_j}^* - \frac{6}{5}g_1^2\delta_{ij}\right], \tag{A.24}$$

$$\gamma_{\bar{Q}} = \frac{1}{16\pi^2}\left[\sum_i Y_{\bar{Q}_i}^* Y_{Q_i} + y_{\bar{u}}^* y_{\bar{u}} + y_{\bar{d}}^* y_{\bar{d}} - \left(\frac{8}{3}g_3^2 + \frac{3}{2}g_2^2 + \frac{1}{30}g_1^2\right)\right], \tag{A.25}$$

$$\gamma_{\bar{u}} = \frac{1}{16\pi^2}\left[\sum_i Y_{u_i}^* Y_{u_i} + 2y_{\bar{u}}^* y_{\bar{u}} - \left(\frac{8}{3}g_3^2 + \frac{8}{15}g_1^2\right)\right], \tag{A.26}$$

$$\gamma_{\bar{d}} = \frac{1}{16\pi^2}\left[\sum_i Y_{d_i}^* Y_{d_i} + 2y_{\bar{d}}^* y_{\bar{d}} - \left(\frac{8}{3}g_3^2 + \frac{2}{15}g_1^2\right)\right], \tag{A.27}$$

$$\gamma_{\bar{L}} = \frac{1}{16\pi^2}\left[\sum_i Y_{L_i}^* Y_{L_i} + y_{\bar{e}}^* y_{\bar{e}} - \left(\frac{3}{2}g_2^2 + \frac{3}{10}g_1^2\right)\right], \tag{A.28}$$

$$\gamma_{\bar{e}} = \frac{1}{16\pi^2}\left[\sum_i Y_{e_i}^* Y_{e_i} + 2y_{\bar{e}}^* y_{\bar{e}} - \frac{6}{5}g_1^2\right], \tag{A.29}$$

$$\gamma_{H_u} = \frac{1}{16\pi^2}\left[3\,\mathrm{Tr}\left(\boldsymbol{y}_u \boldsymbol{y}_u^\dagger\right) + 3y_{\bar{d}}^* y_{\bar{d}} + y_{\bar{e}}^* y_{\bar{e}} - \left(\frac{3}{2}g_2^2 + \frac{3}{10}g_1^2\right)\right], \tag{A.30}$$

$$\gamma_{H_d} = \frac{1}{16\pi^2}\left[\mathrm{Tr}\left(3\boldsymbol{y}_d \boldsymbol{y}_d^\dagger + \boldsymbol{y}_e \boldsymbol{y}_e^\dagger\right) + 3y_{\bar{u}}^* y_{\bar{u}} - \left(\frac{3}{2}g_2^2 + \frac{3}{10}g_1^2\right)\right], \tag{A.31}$$

$$\gamma_\Phi = \frac{1}{16\pi^2}\left[\sum_i \left(6Y_{Q_i}^* Y_{Q_i} + 3Y_{u_i}^* Y_{u_i} + 3Y_{d_i}^* Y_{d_i} + 2Y_{L_i}^* Y_{L_i} + Y_{e_i}^* Y_{e_i}\right) + Y^* Y\right]. \tag{A.32}$$

A.3 A and B terms

The RG equations of SUSY-breaking A and B terms are given by

$$\frac{d\boldsymbol{a}_{u_{ij}}}{d(\log\mu)} = (\gamma_u \boldsymbol{a}_u)_{ij} + (\boldsymbol{a}_u \gamma_Q)_{ij} + \gamma_{H_u}\boldsymbol{a}_{u_{ij}} + 2(\tilde{\gamma}_u \boldsymbol{y}_u)_{ij} + 2(\boldsymbol{y}_u \tilde{\gamma}_Q)_{ij} + 2\tilde{\gamma}_{H_u}\boldsymbol{y}_{u_{ij}}, \tag{A.33}$$

$$\frac{d\boldsymbol{a}_{d_{ij}}}{d(\log\mu)} = (\gamma_d \boldsymbol{a}_d)_{ij} + (\boldsymbol{a}_d \gamma_Q)_{ij} + \gamma_{H_d}\boldsymbol{a}_{d_{ij}} + 2(\tilde{\gamma}_d \boldsymbol{y}_d)_{ij} + 2(\boldsymbol{y}_d \tilde{\gamma}_Q)_{ij} + 2\tilde{\gamma}_{H_d}\boldsymbol{y}_{d_{ij}}, \tag{A.34}$$

$$\frac{d\boldsymbol{a}_{e_{ij}}}{d(\log\mu)} = (\gamma_e \boldsymbol{a}_e)_{ij} + (\boldsymbol{a}_e \gamma_L)_{ij} + \gamma_{H_d}\boldsymbol{a}_{e_{ij}} + 2(\tilde{\gamma}_e \boldsymbol{y}_e)_{ij} + 2(\boldsymbol{y}_e \tilde{\gamma}_L)_{ij} + 2\tilde{\gamma}_{H_d}\boldsymbol{y}_{e_{ij}}, \tag{A.35}$$

$$\frac{da_{\bar{u}}}{d(\log\mu)} = (\gamma_{\bar{u}} + \gamma_{\bar{Q}} + \gamma_{H_d})y_{\bar{u}} + 2(\tilde{\gamma}_{\bar{u}} + \tilde{\gamma}_{\bar{Q}} + \tilde{\gamma}_{H_d})a_{\bar{u}}, \tag{A.36}$$

$$\frac{da_{\bar{d}}}{d(\log\mu)} = (\gamma_{\bar{d}} + \gamma_{\bar{Q}} + \gamma_{H_u})y_{\bar{d}} + 2(\tilde{\gamma}_{\bar{d}} + \tilde{\gamma}_{\bar{Q}} + \tilde{\gamma}_{H_u})a_{\bar{d}}, \tag{A.37}$$

$$\frac{da_{\bar{e}}}{d(\log\mu)} = (\gamma_{\bar{e}} + \gamma_{\bar{L}} + \gamma_{H_u})y_{\bar{e}} + 2(\tilde{\gamma}_{\bar{e}} + \tilde{\gamma}_{\bar{L}} + \tilde{\gamma}_{H_u})a_{\bar{e}}, \tag{A.38}$$

$$\frac{dA_{Q_i}}{d(\log\mu)} = (A_Q \gamma_Q)_i + (\gamma_{\bar{Q}} + \gamma_\Phi)A_{Q_i} + 2(Y_Q \tilde{\gamma}_Q)_i + 2(\tilde{\gamma}_{\bar{Q}} + \tilde{\gamma}_\Phi)Y_{Q_i}, \tag{A.39}$$

$$\frac{dA_{Q_i}}{d(\log\mu)} = (\gamma_u A_u)_i + (\gamma_{\bar{u}} + \gamma_\Phi)A_{u_i} + 2(\tilde{\gamma}_u Y_u)_i + 2(\tilde{\gamma}_{\bar{u}} + \tilde{\gamma}_\Phi)Y_{u_i}, \tag{A.40}$$

$$\frac{dA_{d_i}}{d(\log\mu)} = (\gamma_d A_Q)_i + (\gamma_{\bar{d}} + \gamma_\Phi)A_{d_i} + 2(\tilde{\gamma}_d Y_d)_i + 2(\tilde{\gamma}_{\bar{d}} + \tilde{\gamma}_\Phi)Y_{d_i}, \tag{A.41}$$

$$\frac{dA_{L_i}}{d(\log\mu)} = (A_Q \gamma_L)_i + (\gamma_{\bar{L}} + \gamma_\Phi)A_{L_i} + 2(Y_L \tilde{\gamma}_L)_i + 2(\tilde{\gamma}_{\bar{L}} + \tilde{\gamma}_\Phi)Y_{L_i}, \tag{A.42}$$

$$\frac{dA_{e_i}}{d(\log\mu)} = (\gamma_e A_Q)_i + (\gamma_{\bar{e}} + \gamma_\Phi)A_{e_i} + 2(\tilde{\gamma}_e Y_e)_i + 2(\tilde{\gamma}_{\bar{e}} + \tilde{\gamma}_\Phi)Y_{e_i}, \tag{A.43}$$

$$\frac{dA_Y}{d(\log\mu)} = 3\gamma_\Phi A_Y + 6\tilde{\gamma}_\Phi Y, \tag{A.44}$$

$$\frac{db_H}{d(\log\mu)} = (\gamma_{H_u} + \gamma_{H_d})b_H + 2(\tilde{\gamma}_{H_u} + \tilde{\gamma}_{H_d})\mu_H, \tag{A.45}$$

$$\frac{db_M}{d(\log\mu)} = 2\gamma_\Phi b_M + 4\tilde{\gamma}_\Phi M, \tag{A.46}$$

where the definitions of $\tilde{\gamma}$'s are

$$\tilde{\gamma}_{Q_{ij}} = \frac{1}{16\pi^2}\left[\left(\boldsymbol{y}_u^\dagger \boldsymbol{a}_u + \boldsymbol{y}_d^\dagger \boldsymbol{a}_d\right)_{ij} + Y_{Q_i}^* A_{Q_j} + \left(\frac{8}{3}g_3^2 M_3 + \frac{3}{2}g_2^2 M_2 + \frac{1}{30}g_1^2 M_1\right)\delta_{ij}\right], \tag{A.47}$$

$$\tilde{\gamma}_{u_{ij}} = \frac{1}{16\pi^2}\left[2\left(\boldsymbol{a}_u \boldsymbol{y}_u^\dagger\right)_{ij} + A_{u_i} Y_{u_j}^* + \left(\frac{8}{3}g_3^2 M_3 + \frac{8}{15}g_1^2 M_1\right)\delta_{ij}\right], \tag{A.48}$$

$$\tilde{\gamma}_{d_{ij}} = \frac{1}{16\pi^2}\left[2\left(\boldsymbol{a}_d \boldsymbol{y}_d^\dagger\right)_{ij} + A_{d_i} Y_{d_j}^* + \left(\frac{8}{3}g_3^2 M_3 + \frac{2}{15}g_1^2 M_1\right)\delta_{ij}\right], \tag{A.49}$$

$$\tilde{\gamma}_{L_{ij}} = \frac{1}{16\pi^2}\left[\left(\boldsymbol{y}_e^\dagger \boldsymbol{a}_e\right)_{ij} + Y_{L_i}^* A_{L_j} + \left(\frac{3}{2}g_2^2 M_2 + \frac{3}{10}g_1^2 M_1\right)\delta_{ij}\right], \tag{A.50}$$

$$\tilde{\gamma}_{e_{ij}} = \frac{1}{16\pi^2}\left[2\left(\boldsymbol{a}_e^\dagger \boldsymbol{y}_e\right)_{ij} + A_{e_i} Y_{e_j}^* + \frac{6}{5}g_1^2 M_1 \delta_{ij}\right], \tag{A.51}$$

$$\tilde{\gamma}_{\bar{Q}} = \frac{1}{16\pi^2}\left(\sum_i Y_{Q_i}^* A_{Q_i} + y_{\bar{u}}^* a_{\bar{u}} + y_{\bar{d}}^* a_{\bar{d}} + \frac{8}{3}g_3^2 M_3 + \frac{3}{2}g_2^2 M_2 + \frac{1}{30}g_1^2 M_1\right), \tag{A.52}$$

$$\tilde{\gamma}_{\bar{u}} = \frac{1}{16\pi^2}\left(\sum_i Y_{u_i}^* A_{u_i} + 2y_{\bar{u}}^* a_{\bar{u}} + \frac{8}{3}g_3^2 M_3 + \frac{8}{15}g_1^2 M_1\right), \tag{A.53}$$

$$\tilde{\gamma}_{\bar{d}} = \frac{1}{16\pi^2}\left(\sum_i Y_{d_i}^* A_{d_i} + 2y_{\bar{d}}^* a_{\bar{d}} + \frac{8}{3}g_3^2 M_3 + \frac{2}{15}g_1^2 M_1\right), \tag{A.54}$$

$$\tilde{\gamma}_{\bar{L}} = \frac{1}{16\pi^2}\left(\sum_i Y_{L_i}^* A_{L_i} + y_{\bar{e}}^* a_{\bar{e}} + \frac{3}{2}g_2^2 M_2 + \frac{3}{10}g_1^2 M_1\right), \tag{A.55}$$

$$\tilde{\gamma}_{\bar{e}} = \frac{1}{16\pi^2}\left(\sum_i Y_{e_i}^* A_{e_i} + 2y_{\bar{e}}^* a_{\bar{e}} + \frac{6}{5}g_1^2 M_1\right), \tag{A.56}$$

$$\tilde{\gamma}_{H_u} = \frac{1}{16\pi^2}\left[3\,\mathrm{Tr}\left(\boldsymbol{a}_u \boldsymbol{y}_u^\dagger\right) + 3y_{\bar{d}}^* a_{\bar{d}} + y_{\bar{e}}^* a_{\bar{e}} + \frac{3}{2}g_2^2 M_2 + \frac{3}{10}g_1^2 M_1\right], \tag{A.57}$$

$$\tilde{\gamma}_{H_d} = \frac{1}{16\pi^2}\left[\mathrm{Tr}\left(3\boldsymbol{a}_d \boldsymbol{y}_d^\dagger + \boldsymbol{a}_e \boldsymbol{y}_e^\dagger\right) + 3y_{\bar{u}}^* a_{\bar{u}} + \frac{3}{2}g_2^2 M_2 + \frac{3}{10}g_1^2 M_1\right], \tag{A.58}$$

$$\tilde{\gamma}_\Phi = \frac{1}{16\pi^2}\left[\sum_i \left(6Y_{Q_i}^* A_{Q_i} + 3Y_{u_i}^* A_{u_i} + 3Y_{d_i}^* A_{d_i} + 2Y_{L_i}^* A_{L_i} + Y_{e_i}^* A_{e_i}\right) + Y^* A_Y\right]. \tag{A.59}$$

A.4 Soft scalar masses

We define the following functions to write down the RG equations of soft scalar masses:

$$f(x_1, x_2, x_3; y; z) = \frac{1}{16\pi^2}\left(x_1 y y^\dagger + y y^\dagger x_1 + y x_2 y^\dagger + x_3 y y^\dagger + z z^\dagger\right), \tag{A.60}$$

$$g(a, b, c) = \frac{1}{16\pi^2}\left(\frac{32a}{3}g_3^2|M_3|^2 + 6b g_2^2 |M_2|^2 + \frac{2c^2}{15}g_1^2|M_1|^2\right) - \frac{c}{80\pi^2}g_1^2 S, \tag{A.61}$$

$$S = \mathrm{Tr}\left(\mathbf{m}_Q^2 - 2\mathbf{m}_u^2 + \mathbf{m}_d^2 - \mathbf{m}_L^2 + \mathbf{m}_e^2\right) + m_{H_u}^2 - m_{H_d}^2 - m_{\bar{Q}}^2 + 2m_{\bar{u}}^2 - m_{\bar{d}}^2 + m_{\bar{L}}^2 - m_{\bar{e}}^2, \tag{A.62}$$

where $x_{1,2,3}$ are generally soft scalar masses in generation space and y, z are Yukawa couplings and A parameters with generation indices. The RG equations of soft scalar masses are given by

$$\frac{d\mathbf{m}_Q^2}{d(\log\mu)} = \sum_{x=u,d} f(\mathbf{m}_Q^2, \mathbf{m}_x^2, m_{H_x}^2; \boldsymbol{y}_u^\dagger; \boldsymbol{a}_u^\dagger) + f(\mathbf{m}_Q^2, m_{\bar{Q}}^2, m_\Phi^2; Y_Q; A_Q) - g(1,1,1), \tag{A.63}$$

$$\frac{d\mathbf{m}_u^2}{d(\log\mu)} = 2f(\mathbf{m}_u^2, \mathbf{m}_Q^2, m_{H_u}^2; \boldsymbol{y}_u; \boldsymbol{a}_u) + f(\mathbf{m}_u^2, m_{\bar{u}}^2, m_\Phi^2; Y_u; A_u) - g(1,0,-4), \tag{A.64}$$

$$\frac{d\mathbf{m}_d^2}{d(\log\mu)} = 2f(\mathbf{m}_d^2, \mathbf{m}_Q^2, m_{H_d}^2; \boldsymbol{y}_d; \boldsymbol{a}_d) + f(\mathbf{m}_d^2, m_{\bar{d}}^2, m_\Phi^2; Y_d; A_d) - g(1,0,2), \tag{A.65}$$

$$\frac{d\mathbf{m}_L^2}{d(\log\mu)} = f(\mathbf{m}_L^2, \mathbf{m}_e^2, m_{H_d}^2; \boldsymbol{y}_e^\dagger; \boldsymbol{a}_e^\dagger) + f(\mathbf{m}_L^2, m_{\bar{L}}^2, m_\Phi^2; Y_L; A_L) - g(0,1,-3), \tag{A.66}$$

$$\frac{d\mathbf{m}_e^2}{d(\log\mu)} = 2f(\mathbf{m}_e^2, \mathbf{m}_L^2, m_{H_d}^2; \boldsymbol{y}_e; \boldsymbol{a}_e) + f(\mathbf{m}_e^2, m_{\bar{e}}^2, m_\Phi^2; Y_e; A_e) - g(0,0,6), \tag{A.67}$$

$$\frac{dm_{\bar{Q}}^2}{d(\log\mu)} = f(m_{\bar{Q}}^2, m_{\bar{u}}^2, m_{H_d}^2; y_{\bar{u}}^*; a_{\bar{u}}^*) + f(m_{\bar{Q}}^2, m_{\bar{d}}^2, m_{H_u}^2; y_{\bar{d}}^*; a_{\bar{d}}^*) + f(m_{\bar{Q}}^2, \mathbf{m}_Q^2, m_\Phi^2; Y_Q; A_Q) - g(1,1,-1), \tag{A.68}$$

$$\frac{dm_{\bar{u}}^2}{d(\log\mu)} = 2f(m_{\bar{Q}}^2, m_{\bar{u}}^2, m_{H_d}^2; y_{\bar{u}}; a_{\bar{u}}) + f(m_{\bar{u}}^2, \mathbf{m}_u^2, m_\Phi^2; Y_u; A_u) - g(1,0,4), \tag{A.69}$$

$$\frac{dm_{\bar{d}}^2}{d(\log\mu)} = 2f(m_{\bar{Q}}^2, m_{\bar{d}}^2, m_{H_u}^2; y_{\bar{d}}; a_{\bar{d}}) + f(m_{\bar{d}}^2, \mathbf{m}_d^2, m_\Phi^2; Y_d; A_d) - g(1,0,-2), \tag{A.70}$$

$$\frac{dm_{\bar{L}}^2}{d(\log\mu)} = f(m_{\bar{L}}^2, m_{\bar{e}}^2, m_{H_u}^2; y_{\bar{e}}^*; a_{\bar{e}}^*) + f(m_{\bar{L}}^2, \mathbf{m}_L^2, m_\Phi^2; Y_L; A_L) - g(0,1,3), \tag{A.71}$$

$$\frac{dm_{\bar{e}}^2}{d(\log\mu)} = 2f(m_{\bar{L}}^2, m_{\bar{e}}^2, m_{H_u}^2; y_{\bar{e}}; a_{\bar{e}}) + f(m_{\bar{e}}^2, \mathbf{m}_e^2, m_\Phi^2; Y_e; A_e) - g(0,0,-6), \tag{A.72}$$

$$\frac{dm_{H_u}^2}{d(\log\mu)} = \mathrm{Tr}\left[3f(\mathbf{m}_Q^2, \mathbf{m}_u^2, m_{H_u}^2; \boldsymbol{y}_u^\dagger; \boldsymbol{a}_u^\dagger)\right] + 3f(m_{\bar{Q}}^2, m_{\bar{d}}^2, m_{H_u}^2; y_{\bar{d}}^*; a_{\bar{d}}^*) + f(m_{\bar{L}}^2, m_{\bar{e}}^2, m_{H_u}^2; y_{\bar{e}}^*; a_{\bar{e}}^*) - g(0,1,3), \tag{A.73}$$

$$\frac{dm_{H_d}^2}{d(\log\mu)} = \mathrm{Tr}\left[3f(\mathbf{m}_Q^2, \mathbf{m}_d^2, m_{H_d}^2; \boldsymbol{y}_d^\dagger; \boldsymbol{a}_d^\dagger) + f(\mathbf{m}_L^2, \mathbf{m}_e^2, m_{H_d}^2; \boldsymbol{y}_e^\dagger; \boldsymbol{a}_e^\dagger)\right] + 3f(m_{\bar{Q}}^2, m_{\bar{u}}^2, m_{H_d}^2; y_{\bar{u}}^*; a_{\bar{u}}^*) - g(0,1,-3), \tag{A.74}$$

$$\frac{dm_\Phi^2}{d(\log\mu)} = 12f(m_{\bar{Q}}^2, \mathbf{m}_Q^2, m_\Phi^2; Y_Q; A_Q) + 6f(m_{\bar{u}}^2, \mathbf{m}_u^2, m_\Phi^2; Y_u; A_u) + 6f(m_{\bar{d}}^2, \mathbf{m}_d^2, m_\Phi^2; Y_d; A_d) + 4f(m_{\bar{L}}^2, \mathbf{m}_L^2, m_\Phi^2; Y_L; A_L) + 2f(m_{\bar{e}}^2, \mathbf{m}_e^2, m_\Phi^2; Y_e; A_e) + f(m_\Phi^2, m_\Phi^2, m_\Phi^2; Y; A_Y). \tag{A.75}$$

B Sfermion Mass Matrices in the VMSSM

In the VMSSM, the matter sector has five sets of generations (four copies of the usual generation and one with opposite charges). The quarks and leptons have the 5×5 Dirac mass matrices m_u, m_d and m_e [Eqs. (2.8), (2.9) and (2.10)]. The mass squared matrices of squarks and sleptons, $M^2_{\tilde{u}}$, $M^2_{\tilde{d}}$ and $M^2_{\tilde{e}}$, are 10×10 matrices and that of sneutrinos $M^2_{\tilde{\nu}}$ is a 5×5 matrix, which are given by

$$M^2_{\tilde{u}} = \begin{pmatrix} m_u^\dagger m_u & 0 \\ 0 & m_u m_u^\dagger \end{pmatrix} + \begin{pmatrix} m^2_{\tilde{u}_{LL}} & m^2_{\tilde{u}_{LR}} \\ m^2_{\tilde{u}_{RL}} & m^2_{\tilde{u}_{RR}} \end{pmatrix}, \tag{B.1}$$

$$M^2_{\tilde{d}} = \begin{pmatrix} m_d^\dagger m_d & 0 \\ 0 & m_d m_d^\dagger \end{pmatrix} + \begin{pmatrix} m^2_{\tilde{d}_{LL}} & m^2_{\tilde{d}_{LR}} \\ m^2_{\tilde{d}_{RL}} & m^2_{\tilde{d}_{RR}} \end{pmatrix}, \tag{B.2}$$

$$M^2_{\tilde{e}} = \begin{pmatrix} m_e^\dagger m_e & 0 \\ 0 & m_e m_e^\dagger \end{pmatrix} + \begin{pmatrix} m^2_{\tilde{e}_{LL}} & m^2_{\tilde{e}_{LR}} \\ m^2_{\tilde{e}_{RL}} & m^2_{\tilde{e}_{RR}} \end{pmatrix}, \tag{B.3}$$

$$M^2_{\tilde{\nu}} = m^2_{\tilde{\nu}_{LL}}. \tag{B.4}$$

The diagonal elements of the second matrix in each equation and $m^2_{\tilde{\nu}_{LL}}$ in Eq. (B.4) come from the soft scalar masses and D terms, which are given by

$$m^2_{\tilde{u}_{LL}} = \begin{array}{c} \\ \tilde{u}_{1L} \\ \vdots \\ \tilde{u}_{4L} \\ \tilde{u}_{5L} \end{array} \begin{array}{c} \begin{array}{ccc} \tilde{u}_{1L} & \cdots & \tilde{u}_{4L} \end{array} \quad \tilde{u}_{5L} \\ \begin{pmatrix} & \mathbf{m}^2_Q + \Delta_{\frac{1}{2},\frac{2}{3}} & & 0 \\ & & & \\ & & & \\ & 0 & & m^2_{\bar{u}} + \Delta_{0,-\frac{2}{3}} \end{pmatrix} \end{array}, \tag{B.5}$$

$$m^2_{\tilde{u}_{RR}} = \begin{array}{c} \\ \tilde{u}_{1R} \\ \vdots \\ \tilde{u}_{4R} \\ \tilde{u}_{5R} \end{array} \begin{array}{c} \begin{array}{ccc} \tilde{u}_{1R} & \cdots & \tilde{u}_{4R} \end{array} \quad \tilde{u}_{5R} \\ \begin{pmatrix} & \mathbf{m}^2_u + \Delta_{0,\frac{2}{3}} & & 0 \\ & & & \\ & & & \\ & 0 & & m^2_{\bar{Q}} + \Delta_{-\frac{1}{2},-\frac{2}{3}} \end{pmatrix} \end{array}, \tag{B.6}$$

$$m^2_{\tilde{d}_{LL}} = \begin{array}{c} \\ \tilde{d}_{1L} \\ \vdots \\ \tilde{d}_{4L} \\ \tilde{d}_{5L} \end{array} \begin{array}{c} \begin{array}{ccc} \tilde{d}_{1L} & \cdots & \tilde{d}_{4L} \end{array} \quad \tilde{d}_{5L} \\ \begin{pmatrix} & \mathbf{m}^2_Q + \Delta_{-\frac{1}{2},-\frac{1}{3}} & & 0 \\ & & & \\ & & & \\ & 0 & & m^2_{\bar{d}} + \Delta_{0,\frac{1}{3}} \end{pmatrix} \end{array}, \tag{B.7}$$

$$m^2_{\tilde{d}_{RR}} = \begin{array}{c} \\ \tilde{d}_{1R} \\ \vdots \\ \tilde{d}_{4R} \\ \tilde{d}_{5R} \end{array} \begin{array}{c} \begin{array}{ccc} \tilde{d}_{1R} & \cdots & \tilde{d}_{4R} \end{array} \quad \tilde{d}_{5R} \\ \begin{pmatrix} \mathbf{m}_d^2 + \Delta_{0,-\frac{1}{3}} & & 0 \\ & & \\ 0 & & m^2_{\bar{Q}} + \Delta_{\frac{1}{2},\frac{1}{3}} \end{pmatrix} \end{array}, \tag{B.8}$$

$$m^2_{\tilde{e}_{LL}} = \begin{array}{c} \\ \tilde{e}_{1L} \\ \vdots \\ \tilde{e}_{4L} \\ \tilde{e}_{5L} \end{array} \begin{array}{c} \begin{array}{ccc} \tilde{e}_{1L} & \cdots & \tilde{e}_{4L} \end{array} \quad \tilde{e}_{5L} \\ \begin{pmatrix} \mathbf{m}_L^2 + \Delta_{-\frac{1}{2},-1} & & 0 \\ & & \\ 0 & & m^2_{\bar{e}} + \Delta_{0,1} \end{pmatrix} \end{array}, \tag{B.9}$$

$$m^2_{\tilde{e}_{RR}} = \begin{array}{c} \\ \tilde{e}_{1R} \\ \vdots \\ \tilde{e}_{4R} \\ \tilde{e}_{5R} \end{array} \begin{array}{c} \begin{array}{ccc} \tilde{e}_{1R} & \cdots & \tilde{e}_{4R} \end{array} \quad \tilde{e}_{5R} \\ \begin{pmatrix} \mathbf{m}_e^2 + \Delta_{0,-1} & & 0 \\ & & \\ 0 & & m^2_{\bar{L}} + \Delta_{\frac{1}{2},1} \end{pmatrix} \end{array}, \tag{B.10}$$

$$m^2_{\tilde{\nu}_{LL}} = \begin{array}{c} \\ \tilde{\nu}_{1L} \\ \vdots \\ \tilde{\nu}_{4L} \\ \tilde{\nu}_{5L} \end{array} \begin{array}{c} \begin{array}{ccc} \tilde{\nu}_{1L} & \cdots & \tilde{\nu}_{4L} \end{array} \quad \tilde{\nu}_{5L} \\ \begin{pmatrix} \mathbf{m}_L^2 + \Delta_{\frac{1}{2},0} & & \\ & & \\ 0 & & m^2_{\bar{L}} + \Delta_{\frac{1}{2},0} \end{pmatrix} \end{array}, \tag{B.11}$$

where $\Delta_{T_3,q} = (T_3 - q\sin^2\theta_W)\cos(2\beta)\, m_Z^2$, and T_3 and q are the isospin for SU(2) and the electromagnetic U(1) charge for each field, respectively. The off-diagonal elements of the second matrices in Eqs. (B.1)-(B.3) come from the superpotential and A terms, and are given by

$$m^2_{\tilde{u}_{RL}} = (m^2_{\tilde{u}_{LR}})^\dagger = \begin{array}{c} \\ \tilde{u}_{1R} \\ \vdots \\ \tilde{u}_{4R} \\ \tilde{u}_{5R} \end{array} \begin{array}{c} \begin{array}{ccc} \tilde{u}_{1L} & \cdots & \tilde{u}_{4L} \end{array} \quad \tilde{u}_{5L} \\ \begin{pmatrix} \boldsymbol{a}_{u_{ij}} v_u - \mu_H^* \boldsymbol{y}_{u_{ij}} v_d & & A_{u_i} V + Y_{u_i} Y^* |V|^2 \\ & & \\ A_{Q_i} V + Y_{Q_i} Y^* |V|^2 & & a_{\bar{u}} v_d - \mu_H y_{\bar{u}} v_u \end{pmatrix} \end{array}, \tag{B.12}$$

$$m^2_{\tilde{d}_{RL}} = (m^2_{\tilde{d}_{LR}})^\dagger = \begin{array}{c} \\ \tilde{d}_{1R} \\ \vdots \\ \tilde{d}_{4R} \\ \tilde{d}_{5R} \end{array} \begin{array}{c} \begin{array}{cc} \tilde{d}_{1L} \quad \cdots & \tilde{d}_{4L} \end{array} \quad \tilde{d}_{5L} \\ \begin{pmatrix} & \\ \boldsymbol{a}_{d_{ij}} v_d - \mu_H^* \boldsymbol{y}_{d_{ij}} v_u & A_{d_i} V + Y_{d_i} Y^* |V|^2 \\ & \\ A_{Q_i} V + Y_{Q_i} Y^* |V|^2 & a_{\bar{d}} v_u - \mu_H y_{\bar{d}} v_d \end{pmatrix} \end{array}, \tag{B.13}$$

$$m^2_{\tilde{e}_{RL}} = (m^2_{\tilde{e}_{LR}})^\dagger = \begin{array}{c} \\ \tilde{e}_{1R} \\ \vdots \\ \tilde{e}_{4R} \\ \tilde{e}_{5R} \end{array} \begin{array}{c} \begin{array}{cc} \tilde{e}_{1L} \quad \cdots & \tilde{e}_{4L} \end{array} \quad \tilde{e}_{5L} \\ \begin{pmatrix} & \\ \boldsymbol{a}_{e_{ij}} v_d - \mu_H^* \boldsymbol{y}_{e_{ij}} v_u & A_{e_i} V + Y_{e_i} Y^* |V|^2 \\ & \\ A_{L_i} V + Y_{L_i} Y^* |V|^2 & a_{\bar{e}} v_u - \mu_H y_{\bar{e}} v_d \end{pmatrix} \end{array}. \tag{B.14}$$

References

[1] G. Aad *et al.* [ATLAS Collaboration], Phys. Lett. B **716** (2012) 1 [arXiv:1207.7214 [hep-ex]].

[2] S. Chatrchyan *et al.* [CMS Collaboration], Phys. Lett. B **716** (2012) 30 [arXiv:1207.7235 [hep-ex]].

[3] For a review, H. P. Nilles, Phys. Rept. **110** (1984) 1.

[4] K. Inoue, A. Kakuto, H. Komatsu and S. Takeshita, Prog. Theor. Phys. **68** (1982) 927; L. E. Ibanez and G. G. Ross, Phys. Lett. B **110** (1982) 215; J. R. Ellis, D. V. Nanopoulos and K. Tamvakis, Phys. Lett. B **121** (1983) 123; L. Alvarez-Gaume, J. Polchinski and M. B. Wise, Nucl. Phys. B **221** (1983) 495.

[5] Y. Okada, M. Yamaguchi and T. Yanagida, Prog. Theor. Phys. **85** (1991) 1; H. E. Haber and R. Hempfling, Phys. Rev. Lett. **66** (1991) 1815; J. R. Ellis, G. Ridolfi and F. Zwirner, Phys. Lett. B **257** (1991) 83.

[6] M. Carena, H. E. Haber, S. Heinemeyer, W. Hollik, C. E. M. Wagner and G. Weiglein, Nucl. Phys. B **580** (2000) 29 [hep-ph/0001002].

[7] G. W. Bennett *et al.* [Muon g-2 Collaboration], Phys. Rev. D **73** (2006) 072003 [hep-ex/0602035].

[8] K. Hagiwara, R. Liao, A. D. Martin, D. Nomura and T. Teubner, J. Phys. G **38** (2011) 085003 [arXiv:1105.3149 [hep-ph]].

[9] J. L. Lopez, D. V. Nanopoulos and X. Wang, Phys. Rev. D **49** (1994) 366 [hep-ph/9308336]; T. Moroi, Phys. Rev. D **53** (1996) 6565 [hep-ph/9512396]; M. Carena, G. F. Giudice and C. E. M. Wagner, Phys. Lett. B **390** (1997) 234 [hep-ph/9610233].

[10] S. P. Martin and J. D. Wells, Phys. Rev. D **64** (2001) 035003 [hep-ph/0103067].

[11] M. Endo, K. Hamaguchi, S. Iwamoto, K. Nakayama and N. Yokozaki, Phys. Rev. D **85** (2012) 095006 [arXiv:1112.6412 [hep-ph]].

[12] L. Lavoura and J. P. Silva, Phys. Rev. D **47** (1993) 2046; N. Maekawa, Phys. Rev. D **52** (1995) 1684.

[13] L. Maiani, G. Parisi and R. Petronzio, Nucl. Phys. B **136** (1978) 115 ; S. Theisen, N. D. Tracas and G. Zoupanos, Z. Phys. C **37** (1988) 597; D. Ghilencea, M. Lanzagorta and G. G. Ross, Phys. Lett. B **415** (1997) 253 [hep-ph/9707462].

[14] M. Bando, J. Sato, T. Onogi and T. Takeuchi, Phys. Rev. D **56** (1997) 1589 [hep-ph/9612493].

[15] M. Lanzagorta and G. G. Ross, Phys. Lett. B **349** (1995) 319 [hep-ph/9501394]; T. Kobayashi and K. Yoshioka, Phys. Rev. D **62** (2000) 115003 [hep-ph/0005009].

[16] M. Bando, J. Sato and K. Yoshioka, Prog. Theor. Phys. **98** (1997) 169 [hep-ph/9703321]; M. Bando, T. Kobayashi, T. Noguchi and K. Yoshioka, Phys. Lett. B **480** (2000) 187 [hep-ph/0002102]; Phys. Rev. D **63** (2001) 113017 [hep-ph/0008120].

[17] M. Bando, J. Sato and K. Yoshioka, Prog. Theor. Phys. **100** (1998) 797 [hep-ph/9712530].

[18] B. Pendleton and G. G. Ross, Phys. Lett. B **98** (1981) 291.

[19] H. Georgi and C. Jarlskog, Phys. Lett. B **86** (1979) 297.

[20] T. Moroi and Y. Okada, Mod. Phys. Lett. A **7** (1992) 187; Phys. Lett. B **295** (1992) 73; K. S. Babu, I. Gogoladze and C. Kolda, hep-ph/0410085; K. S. Babu, I. Gogoladze, M. U. Rehman and Q. Shafi, Phys. Rev. D **78** (2008) 055017 [arXiv:0807.3055 [hep-ph]].

[21] S. P. Martin, Phys. Rev. D **81** (2010) 035004 [arXiv:0910.2732 [hep-ph]].

[22] S. R. Coleman and E. J. Weinberg, Phys. Rev. D **7** (1973) 1888.

[23] R. Dermisek and A. Raval, Phys. Rev. D **88** (2013) 013017 [arXiv:1305.3522 [hep-ph]].

[24] A. H. Chamseddine, R. L. Arnowitt and P. Nath, Phys. Rev. Lett. **49** (1982) 970; R. Barbieri, S. Ferrara and C. A. Savoy, Phys. Lett. B **119** (1982) 343; L. J. Hall, J. D. Lykken and S. Weinberg, Phys. Rev. D **27** (1983) 2359.

[25] Y. Okada, M. Yamaguchi and T. Yanagida, Phys. Lett. B **262** (1991) 54.

[26] K. A. Olive *et al.* [Particle Data Group Collaboration], Chin. Phys. C **38** (2014) 090001.

[27] M. Bando and K. Yoshioka, Prog. Theor. Phys. **100** (1998) 1239 [hep-ph/9806400]; Phys. Lett. B **444** (1998) 373 [hep-ph/9810204]; K. S. Babu and J. C. Pati, hep-ph/0203029.

[28] J. Adam *et al.* [MEG Collaboration], Phys. Rev. Lett. **110** (2013) 201801 [arXiv:1303.0754 [hep-ex]].

[29] R. Kitano and K. Yamamoto, Phys. Rev. D **62** (2000) 073007 [hep-ph/0003063].

[30] The ATLAS collaboration, ATLAS-CONF-2015-081; CMS Collaboration [CMS Collaboration], CMS-PAS-EXO-15-004.

[31] L. J. Hall, K. Harigaya and Y. Nomura, arXiv:1605.03585 [hep-ph].